



Review

Recent advances on mixed matrix membranes for CO₂ separation☆

Ming Wang, Zhi Wang*, Song Zhao, Jixiao Wang, Shichang Wang

Chemical Engineering Research Center, School of Chemical Engineering and Technology, Tianjin University, Tianjin 300350, China

Tianjin Key Laboratory of Membrane Science and Desalination Technology, Tianjin 300350, China

State Key Laboratory of Chemical Engineering, Tianjin 300350, China

Collaborative Innovation Center of Chemical Science and Engineering, Tianjin University, Tianjin 300350, China

ARTICLE INFO

Article history:

Received 28 February 2017

Received in revised form 30 June 2017

Accepted 2 July 2017

Available online 22 July 2017

Keywords:

CO₂ separation

Mixed matrix membrane

Material selection

Compatibility

Composite membrane

Future direction

ABSTRACT

Recent advances on mixed matrix membrane for CO₂ separation are reviewed in this paper. To improve CO₂ separation performance of polymer membranes, mixed matrix membranes (MMMs) are developed. The concept of MMM is illustrated distinctly. Suitable polymer and inorganic or organic fillers for MMMs are summarized. Possible interface morphologies between polymer and filler, and the effect of interface morphologies on gas transport properties of MMMs are summarized. The methods to improve compatibility between polymer and filler are introduced. There are eight methods including silane coupling, Grignard treatment, incorporation of additive, grafting, *in situ* polymerization, polydopamine coating, particle fusion approach and polymer functionalization. To achieve higher productivity for industrial application, mixed matrix composite membranes are developed. The recent development on hollow fiber and flat mixed matrix composite membrane is reviewed in detail. Last, the future trend of MMM is forecasted.

© 2017 The Chemical Industry and Engineering Society of China, and Chemical Industry Press. All rights reserved.

1. Introduction

The energy-efficient and environmentally friendly CO₂ separation technology is increasingly necessary and has huge market in industrial application including CO₂ capture, CO₂ removal from flue gas, natural gas treatment and hydrogen purification [1–3]. Membrane-based gas separation is considered as the candidate technology. However, polymer membranes are shown to suffer a permeability–selectivity trade-off limitation [4]. Recently, mixed matrix membranes (MMMs) are developed to overcome the limitation [5–9]. In general, MMMs are fabricated by using two or more different materials of distinct properties. One material (usually a polymer) forms a continuous phase, also known as matrix. Another material forms a dispersed phase, inorganic or organic, which is the so-called filler. The matrix and filler are immiscible and possess different transport properties. There are a larger number of scientific literatures on MMMs for CO₂ separation.

Permeability and selectivity are two important parameters to evaluate membrane performance. For the membranes without a support

membrane or a support layer, permeability is officially called as permeability coefficient (P). It can be expressed as follows:

$$P_i = \frac{Q_i l}{\Delta P_i A} \quad (1)$$

where Q_i is the permeation rate of gas species i at standard temperature and pressure (STP), l is thickness, ΔP_i is the transmembrane partial pressure difference of gas species i , and A is the effective membrane area. The gas permeability coefficient is customarily expressed in the unit of $\text{mol} \cdot \text{m} \cdot \text{m}^{-2} \cdot \text{s}^{-1} \cdot \text{Pa}^{-1}$. However, the permeance (R) is usually applied to assess the permeability for composite membranes and asymmetric membranes. It can be expressed as follows:

$$R_i = \frac{P_i}{l} \quad (2)$$

The gas permeance is customarily expressed in the unit of $\text{mol} \cdot \text{m}^{-2} \cdot \text{s}^{-1} \cdot \text{Pa}^{-1}$.

The selectivity reflects the capability of a membrane to separate one gas from gas mixture. The ideal selectivity ($\alpha_{i/j}^*$) is given by the ratio of the two pure gas permeabilities shown in Eq. (3).

$$\alpha_{i/j}^* = \frac{P_i}{P_j} = \frac{R_i}{R_j} \quad (3)$$

where P_i , R_i , P_j and R_j are the permeability coefficient and permeance of gas species i and j in the membrane, respectively.

☆ Supported by the National Natural Science Foundation of China (21436009) and the Program of Introducing Talents of Discipline to Universities (B06006).

* Corresponding author at: Chemical Engineering Research Center, School of Chemical Engineering and Technology, Tianjin University, Tianjin 300350, China.

E-mail address: wangzhi@tju.edu.cn (Z. Wang).

For permeation of actual i – j mixtures, the mixed gas selectivity, also called as separation factor ($\alpha'_{i/j}$), is calculated by Eq. (4).

$$\alpha'_{i/j} = \frac{y_i/y_j}{x_i/x_j} \quad (4)$$

where y_i and y_j are the molar fraction of gas species i and j in the permeate side, while x_i and x_j are the molar fraction of gas species i and j in the feed side.

2. Material Selection for MMM

As typical MMMs, the polymer acts as a continuous phase and the filler acts as a dispersed phase. To develop high performance MMMs, correct selection of polymer and filler is very important.

2.1. Selection of polymer

In general, gas transport through polymer membranes follows the solution–diffusion mechanism. In such membranes, gas molecules first dissolve in the membranes at the interface of the feed side and the membrane, and then diffuse across the membrane to the permeate side [10]. Permeability is the product of gas solubility and diffusivity. As a result, polymer with specific structure or high affinity for CO₂ molecules can provide high CO₂ permselectivity. However, there are different cases inside facilitated transport polymer membranes. The facilitation of CO₂ transport is accomplished by the “carrier” inside a facilitated transport membrane, which can reversibly react with CO₂ [10]. It is well-known as facilitated transport mechanism or reactivity selective mechanism. At the feed-side interface of the membrane, CO₂ reacts with the carrier and forms a CO₂–carrier reaction product, which diffuses along its concentration gradient to the permeate side of the membrane. Due to a lower CO₂ partial pressure on the permeate side, CO₂ is released from the CO₂–carrier reaction product to the permeate side, while regenerating the carrier that can then react with another CO₂ molecule on the feed side [10]. Hence, a major part of CO₂ is transported by the carriers inside the membranes in addition to the physical solution–diffusion as other non-reactive gases such as N₂, CH₄ and H₂. As a result, both high CO₂ permeability and selectivity can be obtained for facilitated transport polymer membrane materials.

To achieve CO₂ separation, as a continuous phase in MMMs, the polymer should have not only high CO₂ permeability but also high selectivity. For CO₂/N₂ or CO₂/CH₄ separation, because the kinetic diameter of CO₂ molecule is less than that of N₂ or CH₄ molecule (Table 1), diffusivity selectivity of the polymer is higher than one. For CO₂/H₂ separation, because the kinetic diameter of CO₂ molecule is larger than that of H₂ molecule, diffusivity selectivity of the polymer is less than one. To meet high selectivity for CO₂ separation, the polymer should have high solubility selectivity or reactivity selectivity. Hence, the polymer should contain functional groups which only have high affinity for CO₂ molecules or react with CO₂ molecules. Furthermore, the polymer should have high mechanical strength and good thermal stability. Due to the different sources of CO₂, the content, pressure and temperatures vary widely. The polymer should be selected based on practical application conditions. High performance glassy polymers with robust mechanical strength may be applicable for high pressure conditions such as natural

gas purification. Facilitated transport membrane material may be suitable for low pressure flue gas purification, biogas treatment, and hot (>100 °C) syngas separation [11]. Besides, because various kinds of impurity gases such as H₂O, O₂, SO_x, NO_x and H₂S are present as minor components in industrial CO₂ gas feeds, the polymer should have good chemical stability. Finally, the polymer should have good processability. To be employed in large scale applications, the polymer should be capable of being formed into thin membranes with separation layers to achieve high CO₂ permeance.

The common polymers include polyethersulfone (PES) [12–15], polycarbonate (PC) [16], poly(vinyl acetate) (PVAc) [17–19], sulfonated poly(ether ether ketone) (SPEEK) [20,21], poly(2,6-dimethyl-1,4-phenylene oxide) (PPO) [22], cellulose acetate (CA) [23,24], polyimide (PI, such as Matrimid® [25–29]), polyetherimide (such as Ultem [30]), PIM-1 [31–35], poly(ether-block-amide) (Pebax, such as Pebax 1657 [36–39], Pebax 2533 [40] and Pebax 1074 [41]) and poly(vinylamine) (PVAm) [42,43]. The above polymer materials possess different characteristics. PES, PC, SPEEK, PPO, CA, PI, and Ultem are glassy polymers, and have good chemical and thermal stability, permselectivity and processability. PIM-1 is a new kind of glassy polymer. Due to its special ladder-type structure with contorted sites that prevent polymer chains from rotating and packing efficiently, PIM-1 has high free volumes, which results in superior gas separation performance. Pebax as a copolymer has a soft (rubbery) polymer segment such as polyethylene oxide (PEO) and a hard (glassy) polymer segment such as polyamide (PA). On the one hand, PEO soft segment provides enough adhesion between polymer and filler. On the other hand, PEO soft segment has high affinity for CO₂ molecules. PA hard segment provides the mechanical strength. As the facilitated transport membrane material, PVAm containing amine groups exhibits both high permeability and high selectivity through the reversible reactions between reactive carriers – amine groups and CO₂ molecules.

To sum up, Matrimid® is the best polymer for CO₂/CH₄ separation under high pressure, and PVAm is the best polymer for CO₂/N₂, CO₂/CH₄ and CO₂/H₂ separation under low pressure.

2.2. Selection of filler

To achieve CO₂ separation, as a dispersed phase in MMMs, the filler should have high selectivity. The selected filler must exactly correspond to the shape, size and other property difference of the targeted gas molecules, which facilitates CO₂ transport. Furthermore, the selected filler should have good compatibility with polymer matrix. Suitable combination of filler and polymer is a very important factor for improving CO₂ selectivity. Besides, the particle size of the filler should be small. To be employed in industrial applications, separation layer thickness of MMMs is only several micrometers, so the particle size of the filler should be as small as possible.

As a dispersed phase in MMMs, inorganic nanomaterials and organic nanomaterials can both be used as fillers. Inorganic nanofillers used in MMMs can be divided into two classes: solid or impermeable (filled) nanofillers and porous or permeable nanofillers. The impermeable nanofillers include silica and TiO₂. The permeable nanofillers include zeolite, carbon molecular sieve, carbon nanotube, montmorillonite, metal–organic framework, graphene oxide and so on. The critical reviews on nanofillers were made [44–48].

In this section, we critically review the recent progress made in nanofillers. The typical size of the fillers ranges from dozens of nanometers to hundreds of nanometers, and the biggest size of fillers is 20 μm. The typical loading of porous inorganic fillers, laminar inorganic fillers and organic fillers ranges from 10 wt% to 30 wt%, from 1.5 wt% to 6 wt%, and from 15 wt% to 30 wt%, respectively. For most of the porous fillers used in MMMs for CO₂ separation, the pore size ranges from 0.34 nm to 2.6 nm.

For porous filler, the pore size determines CO₂ transport and CO₂ separation mechanism. Generally, CO₂ transport through porous filler

Table 1
Distinctions of gases in size, condensability and reactivity

Gas molecular	Kinetic diameter/nm	Critical temperature/°C	Whether gas molecular reacts with amine or carboxylate groups
CO ₂	0.33	31.05	Yes
N ₂	0.364	–147.05	No
CH ₄	0.38	–82.45	No
H ₂	0.289	–239.85	No

follows molecular sieving mechanism and surface diffusion mechanism. When the pore size of the porous filler is roughly the same as kinetic diameter of the permeating gas molecule, gas transport through porous filler follows molecular sieving mechanism [49]. If the pore size of the porous filler is between the diameters of the CO₂ and other gas molecules, only the smaller gas molecule can permeate through the porous filler leading to a more efficient separation. When the pore size of the porous filler increases, if the gas molecule exhibits a strong affinity for the filler surface and adsorption along the pore walls, gas transport through porous filler follows surface diffusion mechanism [49]. Efficient CO₂ separation can take place by this mechanism due to differences in the amount of adsorption of the CO₂ and other gas molecules. When the pore size of the porous filler is big enough, molecular sieving and surface diffusion mechanisms often coexist. For the laminar inorganic fillers, interlamellar spacing determines CO₂ transport and CO₂ separation mechanism. In general, CO₂ transport through galleries between the neighboring nanosheets follows molecular sieving mechanism.

Effect of the fillers on CO₂ separation performance of MMMs is summarized in Table 2. The fillers not only disturb polymer chain packing and increase free volume, but also facilitate CO₂ transport by itself, which results in improvement of membrane performance. The fillers are reviewed in the section in detail.

2.2.1. Carbon–silica nanocomposite materials

Carbon–silica nanocomposite materials (CSMs) have a tunable porosity and surface chemistry which is controlled by the carbon deposition, the pyrolysis conditions and post-synthetic treatments. The carbon fraction of such nanocomposite fillers increases the affinity for CO₂.

Anjum *et al.* [50] developed MMMs by adding porous CSM fillers to Matrimid® matrix. Owing to the addition of a carbon phase, providing an increased affinity for the CO₂ molecules next to the creation of extra porosity and free volume, the overall separation efficiency of MMMs increased.

2.2.2. Graphene oxide

The effective gas separation for graphene oxide (GO) is based on the formation of the molecular sieving galleries between the neighboring nanosheets or possible defects on the nanosheets.

Dong *et al.* blended the partially porous reduced graphene oxide (PRG) nanosheets into Pebax 1657 polymer to prepare MMMs [39]. For PRG, the narrow gas flow galleries (average width of 0.34 nm) between the neighboring nanosheets ensured effective molecular sieving of CO₂ against other larger gas molecules, while the mesoscopic pores on the laminate provided rapid gas transport pathways. Hence, the MMMs had substantially improved CO₂ permeability as well as CO₂/N₂ selectivity.

2.2.3. Attapulgite

Attapulgite (ATP) is one kind of natural clay with low cost and high availability. In view of its narrow size of the tunnel-like rectangular microspores (0.37 nm × 0.60 nm), ATP is anticipated to distinguish CO₂ (0.33 nm) from N₂ (0.364 nm).

Xiang *et al.* blended Pebax 1657 and ATP nanorods to fabricate MMMs [51]. Both the CO₂ permeability and CO₂/N₂ selectivity of the MMMs increased at low ATP loadings (<6.3 wt%). Compared with the pristine Pebax membrane, CO₂ permeability and CO₂/N₂ selectivity of the MMMs with 1.7 wt% ATP increased by 37.5% and 30%, respectively.

2.2.4. Metal–organic frameworks

Metal–organic frameworks (MOFs) are a large emerging class of hybrid materials with porous crystalline structures, and combine the connectivity of metal centers with the bridging ability of organic ligands. Careful choice of metal and linker allows MOFs to be designed and synthesized with the desired functionalities, pore sizes and pore shapes.

Cu-BTC is made of copper clusters linked to each other via trimesic acid. Cu-BTC consists of main channels of a square cross-section of ~0.9 nm diameter and tetrahedral side pockets of ~0.5 nm, which are connected to the main channels by triangular windows of ~0.35 nm diameter. Ge *et al.* [22] developed MMMs by incorporating size-reduced Cu-BTC in poly(2,6-dimethyl-1,4-phenylene oxide) (PPO) matrix, and demonstrated that the incorporation of the Cu-BTC led to the improvement of both gas permeability and selectivity. *sod*-ZMOF has micropores of approximate 0.96 nm. For CO₂/light gas mixture, molecular sieving does not happen through *sod*-ZMOF due to the large micropores. However, *sod*-ZMOF has high affinity for CO₂. Kılıç *et al.* [52] fabricated Matrimid-*sod*-ZMOF MMMs, and found that with increasing *sod*-ZMOF, both CO₂ permeability and selectivity of the MMMs increased.

MIL-53 has open pores of diameter 0.85 nm at room temperature. MIL-53 was added to Matrimid® and poly(4-methyl-1-pentene) (PMP) for CO₂/CH₄ and CO₂/H₂ separation, respectively [27,53]. MIL-53 with polar functional groups is selected as filler. Rodenas *et al.* [54] fabricated MMMs by incorporating NH₂-functionalized MIL-53(Al) in PI.

MIL-101(Cr) exhibits two types of cages: small cages, which possess a free diameter of 2.9 nm and pentagonal windows of 1.2 nm, and larger cages with a free diameter of 3.4 nm and both pentagonal and hexagonal windows, the latter with a 1.45 nm by 1.6 nm free aperture. Naseri *et al.* [55] prepared the Matrimid-MIL-101 MMMs. Compared with the neat Matrimid® membrane, CO₂/CH₄ and CO₂/N₂ ideal selectivities of the MMMs increased. MIL-101 with polar functional groups is selected as filler. Xin *et al.* [21] modified MIL-101(Cr) by concentrated sulfuric acid and trifluoromethanesulfonic anhydride to prepare sulfonated MIL-101(Cr) [S-MIL-101(Cr)], and then incorporated the S-MIL-101(Cr) into SPEEK to prepare MMMs. The addition of the S-MIL-101(Cr) increased the CO₂/CH₄ and CO₂/N₂ selectivity of the MMMs due to the increased CO₂ solubility. Seoane *et al.* [56] developed MMMs by dispersing amino functionalized MOFs (NH₂-MIL-53(Al) or NH₂-MIL-101(Al)) in sulfur-containing copolyimide. Rodenas *et al.* [57] prepared MMMs by dispersing NH₂-MIL-53(Al) and NH₂-MIL-101(Al) in polysulfone (PSf) and PI, and found that the incorporation of the MOF fillers had a positive effect on the separation performance.

MIL-125 has a quasi-cubic tetragonal structure in which the octahedral (1.07 nm) and tetrahedral (0.47 nm) cages are accessible through a window of about 0.5–0.7 nm. Guo *et al.* [58] fabricated MMMs by incorporating NH₂-MIL-125 into PSf matrix, and demonstrated that the incorporation of NH₂-MIL-125(Ti) particles could significantly improve the CO₂ permeability, and slightly enhance CO₂/CH₄ separation factor. Anjum *et al.* [29] added MIL-125(Ti) and the amine-functionalized counterpart (NH₂-MIL-125) as fillers to Matrimid® polyimide. The synthesized MMMs had the good adhesion between the fillers and the polymer matrix, and the NH₂-functionalized filler was preferred as it led to higher selectivities and permeabilities.

UiO-66 can exhibit strong affinity for CO₂ molecules owing to the —OH groups coordinated to Zr cluster, and triangular windows possess the size of 0.6 nm. Shen *et al.* [59] embedded CO₂-philic zirconium metal organic framework UiO-66 and UiO-66-NH₂ nanocrystals into Pebax membranes. The hydrogen bonding frameworks between UiO-66-NH₂ and Pebax were enhanced. The as-prepared Pebax–UiO-66-NH₂ MMM with MOF loading of 10 wt% displayed a CO₂ permeability of $4.36 \times 10^{-14} \text{ mol} \cdot \text{m} \cdot \text{m}^{-2} \cdot \text{s}^{-1} \cdot \text{Pa}^{-1}$ and CO₂/N₂ selectivity of 72.

MOFs with hydroxyl groups are selected as fillers. Mg-MOF-74 exhibits exceptionally high CO₂ selective adsorption over CH₄ and 1-D hexagonal channels of 1.1 nm diameter. Tien-Binh *et al.* [34] added a novel filler having hydroxyl functional groups on the surface (Mg-MOF-74) to PIM-1. Under optimized conditions, chemical crosslinking between the hydroxyl groups and the fluoride chain-ends of PIM-1 was facilitated to completely remove interfacial defects. Compared with the neat PIM-1 membrane, CO₂ permeability of the MMMs with 20 wt% MOF-74 increased by 3.2 times to $7.12 \times 10^{-12} \text{ mol} \cdot \text{m} \cdot \text{m}^{-2} \cdot \text{s}^{-1} \cdot \text{Pa}^{-1}$, meanwhile CO₂/CH₄ selectivity was improved to 19.1.

Table 2
Effect of fillers on CO₂ separation performance of MMMs

Type of filler	Filler ^①	Particle size/nm	Pore size/nm	Loading/wt%	Polymer ^②	Feed gas	Operation conditions	CO ₂ permeability ×10 ⁻¹⁴ /mol·m·m ⁻² ·s ⁻¹ ·Pa ⁻¹	CO ₂ /N ₂ selectivity	CO ₂ /CH ₄ selectivity	CO ₂ /H ₂ selectivity	Ref.
Inorganic	CSM-18.4	~520 ± 140	1.54	30	Matrimid [®]	CO ₂ /N ₂ (50:50, v/v)	35 °C, 0.9 MPa	1.32	38.1	–	–	[50]
	CSM-23.3	~520 ± 140	1.48	30	Matrimid [®]	CO ₂ /CH ₄ (50:50, v/v)	35 °C, 0.9 MPa	1.30	–	41.9	–	[50]
	PRG	–	11.95	~5	Pebax [®]	CO ₂ /N ₂ (50:50, v/v)	35 °C, 0.9 MPa	1.76	37.8	–	–	[39]
	ATP	Length: 500–1500 Width: 30–50	0.66	1.7	Pebax [®]	Pure gases	30 °C, 0.2 MPa	3.99	104	–	–	[51]
	Cu-BTC-S1	13000	–	10	PPO	Pure gases	35 °C, 1.0 MPa	3.48	84	–	–	[22]
	Cu-BTC-S2	6000	–	10	PPO	Pure gases	30 °C	~2.85	~18.5	~23.5	~1.0	[52]
	Sod-ZMOF	2000–20000	0.96	5.10, 20	Matrimid [®]	CO ₂ /CH ₄ (50:50 mol/mol)	35 °C, 0.4 MPa	~2.88	~23.5	~28.5	~1.0	[52]
	MIL-53	123.4, 466.8	–	15	Matrimid [®]	Pure gases	0.3 MPa	0.23–0.46	–	36.6–43.4	–	[27]
	MIL-53	100	0.91	30	PMP	Pure gases	30 °C, 0.8 MPa	0.42	–	51.8	–	[53]
	NH ₂ -MIL-53	~1000	–	25	Matrimid [®]	CO ₂ /CH ₄ (50:50, mol/mol)	30 °C, 0.3 MPa	12.64	–	–	24.96	[54]
	MIL-101	<1000	–	10	Matrimid [®]	Pure gases	35 °C, 1.0 MPa	~0.49	–	~35	–	[55]
	S-MIL-101(Cr)	~550	0.5–2.6	40	SPEEK	Pure gas	30 °C, 0.1 MPa, in humidified state	69.14	52.92	55.77	–	[21]
	NH ₂ -MIL-101(Al)	104 ± 28	–	10	P1	CO ₂ /N ₂ (20:80, v/v)	30 °C, 0.1 MPa, in humidified state	1.11	40	–	–	[56]
	MW-NH ₂ -MIL-101(Al)	~1000	–	8.15, 25	PSF	CO ₂ /CH ₄ (1:1)	35 °C, 0.3 MPa	2.38	–	41.6	–	[57]
	MIL-125	1500–2000	–	15.30	Matrimid [®]	CO ₂ /CH ₄ (1:1)	35 °C, 0.3 MPa	5.03	–	29.6	–	[29]
	NH ₂ -MIL-125	<1500–2000	–	15.30	Matrimid [®]	CO ₂ /CH ₄ (50:50, mol/mol)	0.9 MPa	~0.18–0.28	–	~24–29.0	–	[58]
	NH ₂ -MIL-125(Ti)	Length: 1000 Width: 500	–	10, 20, 30	PSF	CO ₂ /CH ₄ (50:50, mol/mol)	0.9 MPa	~0.35, ~0.32	–	~35, ~36	–	[59]
	UIO-66	60–80	0.6	10	Pebax [®]	CO ₂ /N ₂ (50:50, v/v)	25 °C, 0.3 MPa, in humidified state	0.60, 0.90	–	44.37	–	[60]
	UIO-66-NH ₂	60–80	0.59	10	Pebax [®]	CO ₂ /N ₂ (50:50, v/v)	25 °C, 0.2 MPa, in humidified state	0.57, 1.68	–	50.37	–	[61]
Organic	MOF-74	10000–15000	1.08	10, 15, 20	PIM-1	Pure gas	35 °C, 0.35 MPa	0.62–1.34	–	28.3–29.2	–	[62]
	ZIF-71	–	–	20	UV-PIM	CO ₂ /CH ₄ (50:50, mol/mol)	35 °C, 0.3 MPa	74.51	–	32.8	–	[63]
	ZIF-8	<80	–	20	6FDA-Durene/DABA (9/1)	CO ₂ /CH ₄ (30:70, mol/mol)	35 °C, 0.2 MPa	63.80	–	32.2	–	[64]
	ZIF-8	–	–	5.10, 15, 20, 25, 30, 35	Pebax [®]	CO ₂ /CH ₄ (50:50)	35 °C, 0.2 MPa	24.39	–	19.61	–	[40]
	ZIF-8	100–200	–	3.5, 7, 10, 15, 20, 30	6FDA-Durene	Pure gas	25 °C, 0.2 MPa	12.23–43.11	–	8.1–9.0	–	[65]
	ZIF-8(S)	88	–	30	SEBS	Pure gas	25 °C, 0.2 MPa	53.38–73.21	–	21.9–17.1	–	[66]
	ZIF-8(M)	240	–	–	–	Pure gas	25 °C	14.71	10.6	5.2	–	[67]
	ZIF-8(L)	533	–	–	–	Pure gas	25 °C	15.23	12.0	5.4	–	[68]
	H-ZIF-8	721 ± 36	–	10, 20, 30	PVC-g-POEM	Pure gas	35 °C	15.59	10.8	5.2	–	[69]
	ZIF-11	500–5000	–	10–70	Pebax [®]	Pure gas	20 °C, 0.2 MPa	5.70–20.87	–	12.2–11.2	–	[70]
	CNTs/GO	–	–	5/5	Matrimid [®]	Pure gas	30 °C, 0.2 MPa	6.90–13.50	52.96–29.0	9.50–12.49	8.0–2.5	[71]
	ZIF-8@GO-6	–	–	6	Pebax [®]	Pure gas	25 °C, 0.1 MPa	1.28	81	84.60	–	[72]
	PANI nanosheet	Thickness: 40–60	–	17	PVAm	CO ₂ /N ₂ (20:80 v/v)	25 °C, 0.11 MPa, in humidified state	8.34	47.6	–	–	[73]
	PANI nanorod	Diameter: 50 Length: 160	–	17	PVAm	CO ₂ /N ₂ (15:85 v/v)	25 °C, 0.11 MPa, in humidified state	40.20 × ^③	120	–	–	[74]
	NHs	~250	–	5.10, 15, 20	Matrimid [®]	Pure gas	30 °C, 0.2 MPa, in humidified state	53.67 ^③	240	–	–	[75]
	CANs	400	–	5.10, 15, 20, 30	Pebax [®]	Pure gas	25 °C, 0.2 MPa, in humidified state	4.56–9.31	43–52	52–61	–	[76]
	PEGSS	350–420	–	20	Matrimid [®]	Pure gas	25 °C, 0.2 MPa, in humidified state	29.82–67.87	56–85	19–33	–	[77]
	HCP	55	–	16.67	PIM-1	Pure gas	30 °C, 0.1 MPa	0.28	61.24	50.29	–	[78]
						Pure gas	25 °C, 0.2 MPa	334.06	20.27	–	–	[79]

^① CSM: carbon-silica nanocomposite materials, PRG: porous reduced graphene oxide, ATP: attapulgite, GO: graphene oxide, PANI: polyaniline, NHs: nanohydrogels, CANs: carboxylic acid nanogels, PEGSS: poly(ethylene glycol)-containing polymeric submicrospheres, HCP: hypercrosslinked polystyrene.

^② PPO: poly(2,6-dimethyl-1,4-phenylene oxide), PMP: poly(4-methyl-1-pentene), SPEEK: sulfonated poly(ether ether ketone), P1: sulfur-containing copolyimides (6FDA:DSDA/4MPD:4,4'-ODA 1:1), P2: sulfur-containing copolyimides (6FDA/4MPD:4,4'-ODA 1:1), PSF: polysulfone, UV-PIM: UV treated PIM, SEBS: polystyrene-block-poly(ethylene-ran-butylene)-block-polystyrene, PVC-g-POEM: poly(vinyl chloride)-g-poly(oxyethylene methacrylate), PVAm: poly(vinylamine).

^③ Permeability is calculated by permeance multiplied by the separation layer thickness, *l*: the separation layer thickness, μm .

2.2.5. Zeolite imidazolate frameworks

Zeolite imidazolate frameworks (ZIFs) are built of tetrahedral metal ions (e.g., Zn, Co) bridged by imidazoles. ZIFs have permanent porosity, and relatively high thermal and chemical stability, which makes them attractive candidates for nanofiller used in MMMs.

ZIF-71 has its rhombic structure with an aperture size of 0.42 nm and a pore cavity of 1.65 nm. Hao *et al.* [60] developed MMMs consisting of a zeolite imidazolate framework-71 (ZIF-71, $\text{Zn}(\text{cbIm})_2$) and PIM-1 with and without UV irradiation, and found that the addition of ZIF-71 considerably enhanced the gas permeability without compromising the gas pair selectivities of CO_2/N_2 and CO_2/CH_4 , and the UV treated MMM with 20 wt% ZIF-71 had a CO_2 permeability of around $6.38 \times 10^{-13} \text{ mol} \cdot \text{m} \cdot \text{m}^{-2} \cdot \text{s}^{-1} \cdot \text{Pa}^{-1}$ and a CO_2/CH_4 selectivity of 32.2 under mixed gas tests.

ZIF-8 has large (1.16 nm) pore cavities that are accessible through small (0.34 nm) pore apertures, which complement the kinetic diameter of CO_2 (0.33 nm), allowing for CO_2 separation via a sieving mechanism. Askari and Chung [61] fabricated MMMs by directly mixing ZIF-8 suspension into three 4,4'-(hexafluoroisopropylidene) diphthalic anhydride (6FDA)-based polyimide solutions, and the MMM made of 6FDA-Durene/DABA (9/1) and 20 wt% ZIF-8 displayed an impressive CO_2 permeability of $2.44 \times 10^{-13} \text{ mol} \cdot \text{m} \cdot \text{m}^{-2} \cdot \text{s}^{-1} \cdot \text{Pa}^{-1}$ and a CO_2/CH_4 selectivity of 19.61 in mixed gas tests. Bushell *et al.* developed MMMs consisting of PIM-1 and ZIF-8, and found that an increase in ZIF-8 loading led to increases in the permeability as well as in the separation factors, and data points on several Robeson diagrams were located above the 2008 upper bound. Nafisi and Hägg [40] developed MMMs by using ZIF-8 as inorganic filler in Pebax 2533 polymer matrix. As the inorganic filler content increased, the permeability of all examined gases increased. Nafisi and Hägg [62] also added ZIF-8 to 6FDA-Durene PI. Chi *et al.* [63] prepared MMMs consisting of polystyrene-block-poly(ethylene-ran-butylene)-block-polystyrene (SEBS) block copolymers and size-controlled ZIF-8 nanoparticles to investigate the effect of filler particle size on MMM gas separation performance, and found that ZIF-8(M) (240 nm) was the most effective in improving gas permeability and selectivity.

Hwang *et al.* [64] fabricated MMMs by dispersing hollow zeolite imidazole frameworks (H-ZIF) filler in poly(vinyl chloride)-g-poly(oxyethylene methacrylate) (PVC-g-POEM) graft copolymer matrix. Compared with pure PVC-g-POEM membranes, the MMMs exhibited an 8.9-fold increase in CO_2 permeability with only a small decrease in CO_2/CH_4 selectivity.

ZIF-11 has cages with diameter of 1.46 nm which are connected via apertures with diameter of 0.3 nm. Ehsani and Pakizeh [65] incorporated ZIF-11 into Pebax® 2533 polymer in the range of 10wt%-70 wt% to fabricate MMMs. Excellent adhesion existed between ZIF-11 and polymer matrix, especially at 30 wt% loading. However, at 50 and 70 wt% ZIF-11 loadings, a few voids were observed throughout the membranes.

2.2.6. Two-component fillers

Except for single kinds of inorganic nanoparticle as filler, two kinds of inorganic nanoparticles can be added together as two-component fillers. Li *et al.* [66] prepared MMMs by incorporating carbon nanotubes (CNTs) and GO into a Matrimid® matrix. The extraordinary smooth walls of CNTs acted as a highway to render high permeability, whereas the GO nanosheets acted as a selective barrier to render high selectivity through the hydroxyl and carboxyl groups on GO surface in MMMs. The MMM with 5 wt% CNTs and 5 wt% GO displayed the optimum performance with a CO_2 permeability of $1.28 \times 10^{-14} \text{ mol} \cdot \text{m} \cdot \text{m}^{-2} \cdot \text{s}^{-1} \cdot \text{Pa}^{-1}$, a CO_2/CH_4 selectivity of 84.60 and a CO_2/N_2 selectivity of 81.00. Furthermore, the composites consisting of two kinds of inorganic nanoparticles can be also used as two-component fillers. Dong *et al.* [67] fabricated MMMs by incorporating ZIF-8@GO composites into Pebax matrix. On the one hand, the high-aspect ratio GO nanosheets in polymer matrix increased the length of the tortuous path of gas diffusion, which enhanced the

diffusivity selectivity. On the other hand, the inherent high permeability of ZIF-8 with ultra-microporosity could enhance the gas permeability and solubility selectivity of MMMs. The MMM containing 6 wt% ZIF-8@GO exhibited the optimum performance with a CO_2 permeability of $8.34 \times 10^{-14} \text{ mol} \cdot \text{m} \cdot \text{m}^{-2} \cdot \text{s}^{-1} \cdot \text{Pa}^{-1}$ and a CO_2/N_2 selectivity of 47.6.

Compared with inorganic nanofillers, organic nanofillers are emerging fillers. Organic nanofillers have advantages such as improved adhesion to polymer matrix. This superiority may be attributed to the organic feature of the filler. In addition, some organic nanofillers can provide unique properties. For instance, nanohydrogels can absorb and retain extremely high water content, and the incorporation of nanohydrogels in MMMs can increase water uptake of MMMs, which is beneficial to facilitating CO_2 transport.

Mixed matrix material with organic nanofillers and polymer blends are both important membrane materials for CO_2 separation. Polymer blends can be categorized as miscible and phase-separated blends (immiscible and partially miscible blends) [73]. In miscible blends, both the polymers are dissolved in each other at molecular levels representing a homogeneous single-phase behavior. However, in phase-separated blends both the polymers are not dissolved in each other and are separated by an interface between the two phases [74]. Hence, mixed matrix material with organic nanofillers should be phase-separated blends. Its performance is strongly dependent on interface morphology, specific volume fraction, and size and shape of the dispersed and continuous phase [74]. In many cases, mixed matrix material with organic nanofillers is beneficial to CO_2 transport compared with miscible blends. It is mainly attributed to suitable interface morphology between two phases and the specific structure of dispersed phase such as pore size and functional groups.

Organic nanofillers used in the MMMs include polyaniline [68,69], poly(*N*-isopropylacrylamide) nanohydrogels [70], carboxylic acid nanogels [71], poly(ethylene glycol)-containing polymeric submicrospheres [72], and hypercrosslinked polystyrene [33]. The organic nanofillers are reviewed in the following sections.

2.2.7. Polyaniline

The incorporation of polyaniline (PANI) disturbs chain packing, and increases fractional free volume. Moreover, PANI with amine groups can facilitate CO_2 transport through reversible reaction between amine groups and CO_2 molecules, which results in the improvement of membrane performance [68,69].

2.2.8. Nanohydrogels

The addition of nanohydrogels increases the fractional free volume, water uptake and water retention capacity of the MMMs, which is beneficial to improving CO_2 separation performance of polymer membranes.

Li *et al.* [70] incorporated poly(*N*-isopropylacrylamide) nanohydrogels (NHs) into Matrimid® to prepare MMMs. The NHs homogeneously embedded in the Matrimid® matrix acted as water reservoirs to not only provide more water for dissolving CO_2 , but also construct interconnected CO_2 transport passageways. The as-prepared Matrimid-NHs-20 membrane exhibited CO_2/CH_4 and CO_2/N_2 selectivities of 61 and 52 with a CO_2 permeability of $9.31 \times 10^{-14} \text{ mol} \cdot \text{m} \cdot \text{m}^{-2} \cdot \text{s}^{-1} \cdot \text{Pa}^{-1}$. Li *et al.* [71] added carboxylic acid nanogels (CANs) into Pebax 1657 to fabricate MMMs. The incorporation of CANs simultaneously tailored favorable water environment and increased CO_2 transport sites within the membranes. The Pebax-CANs-30 membrane displayed CO_2/CH_4 and CO_2/N_2 selectivities of 33 and 85 with a CO_2 permeability of $6.79 \times 10^{-13} \text{ mol} \cdot \text{m} \cdot \text{m}^{-2} \cdot \text{s}^{-1} \cdot \text{Pa}^{-1}$.

2.2.9. Poly(ethylene glycol)-containing polymeric submicrospheres

Wang *et al.* [72] incorporated poly(ethylene glycol) (PEG)-containing polymeric submicrospheres (PEGSS) into PI to prepare MMMs. The favorable affinity between PEGSS and CO_2 greatly increased CO_2 solubility, which led to an increase in CO_2 permeability. Compared with those of pristine PI membrane, CO_2 permeability and CO_2/N_2 selectivity

of the PI-PEGSS(20) membrane with 20 wt% PEGSS increased by 35% and 104%, respectively.

2.2.10. Hypercrosslinked polystyrene

Mitra *et al.* [33] added hypercrosslinked polystyrene (HCP) into PIM-1 to fabricate MMMs. Because the nanosized HCP possessed rigid nanoporous structure, the addition of the HCP not only led to higher permeability but also to a significant arrest in polymer aging and permeability loss.

To sum up, in view of selectivity, compatibility and particle size, PANI is the best filler for CO₂/N₂ separation, NHs is the best filler for CO₂/CH₄ separation, and MIL-53 is the best filler for CO₂/H₂ separation.

3. Interface Morphologies

Interface morphology is a determinant factor for the overall transport property. Fig. 1 displays a schematic diagram of various nanoscale structures at the polymer/filler interface [5]. Case 1 shows an ideal morphology. Case 2 represents the detachment of polymer chains from the filler surface, causing the interface voids. Case 3 displays that the polymer chains in direct contact with the filler surface can be rigidified compared to the bulk polymer chains. Case 4 indicates a situation in which the surface pores of the filler have been partially sealed by the rigidified polymer chains.

When there is a poor compatibility between polymer matrix and filler, Case 2 appears. Due to the less resistance in interface voids, gas transports through interface voids instead of polymer matrix or filler, which improves gas permeability. Meanwhile, change on gas selectivity is dependent on the size of interface voids. Generally, gas selectivity decreases. In other words, as gas molecules take this non-selective and less resistant by-pass instead passing through pores in the filler, membrane performance deteriorates more or less. When there is a very good compatibility between polymer matrix and filler, Case 3 and Case 4 occur. If Case 3 happens, the movement of polymer chain at polymer/filler interface is restrained, which reduces gas adsorption, and then reduces gas permeation. Hence, gas permeability decreases, but an increase in gas selectivity is not obvious. If Case 4 happens, because pores of the filler are partially sealed, gas permeability declines.

In order to discuss the structure–property relationship of the MMMs conveniently, interface morphologies can be roughly divided into two

classes: there are interface voids and there are no interface voids. Based on this, Wang *et al.* [75] systematically analyzed the relationship between polymer–filler interfaces and gas transport properties of the MMMs with different nanofillers. As shown in Fig. 2, considering interface morphology, types of nanofillers and distribution of nanofillers in membrane, ten kinds of possible separation layer structures of MMMs were proposed, and their corresponding gas transport pathways were discussed. Moreover, for each case, the change on gas permeance of the MMMs with increasing feed pressure was analyzed. If the size of interface voids was larger than the mean free path of the gas molecules, and the interconnectivity of interface voids formed interface void channels across the separation layer of the MMM, viscous flow could occur, which led to an increase in gas permeance and a decrease in gas selectivity with increasing feed pressure. Conversely, when viscous flow could not occur for N₂, O₂ or CH₄ transport through nanofillers, an increase in gas permeance of the MMMs with increasing feed pressure demonstrated that there were void channels between polymer phase and nanofiller phase and the size of interface voids was larger than the mean free path of the gas molecules.

4. Methods to Improve Compatibility

Generally, there is poor compatibility between glassy polymer and filler, which results in a decrease in gas selectivity. To avoid interface void and improve membrane performance, researchers adopt the following eight methods to improve interface compatibility.

4.1. Silane coupling

Organofunctional silanes as the most prominent members of coupling agents can be hydrolyzed to form silanol groups. These silanol groups then react with the hydroxyl groups on the surface of inorganic filler during condensation reaction to form stable siloxane bonds. By introducing the silylated inorganic fillers into a polymeric matrix, the dual reactivity of silicone in organosilane serves as bridges between fillers and matrix.

Sanaeepur *et al.* [76] modified micro-sized nanoporous sodium zeolite-Y (NaY) by 3-aminopropyl(diethoxy)methylsilane (APDEMS), and incorporated the silylated particles into a homogeneous CA membrane to achieve better polymer–zeolite adhesion in MMMs.

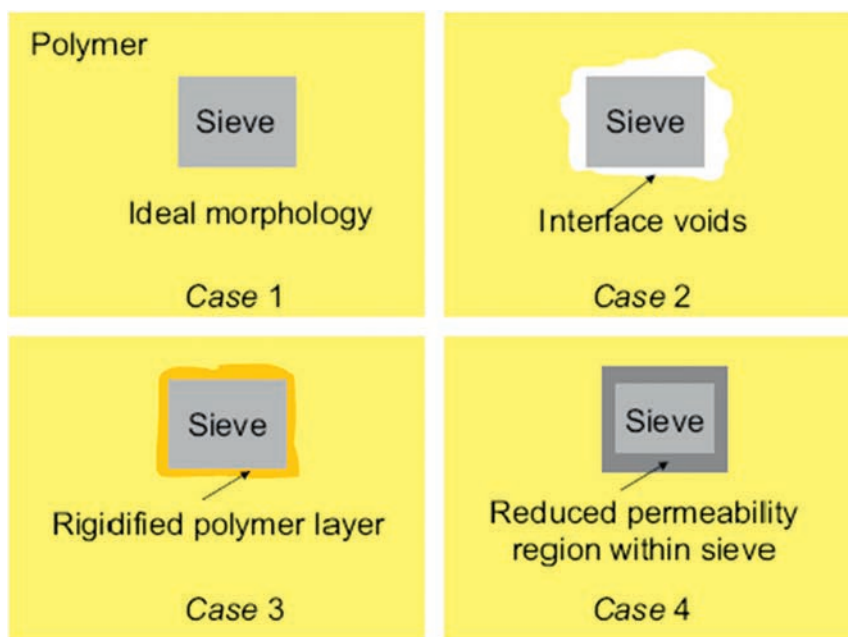


Fig. 1. The schematic diagram of various nanoscale morphology of the mixed matrix structure [5].

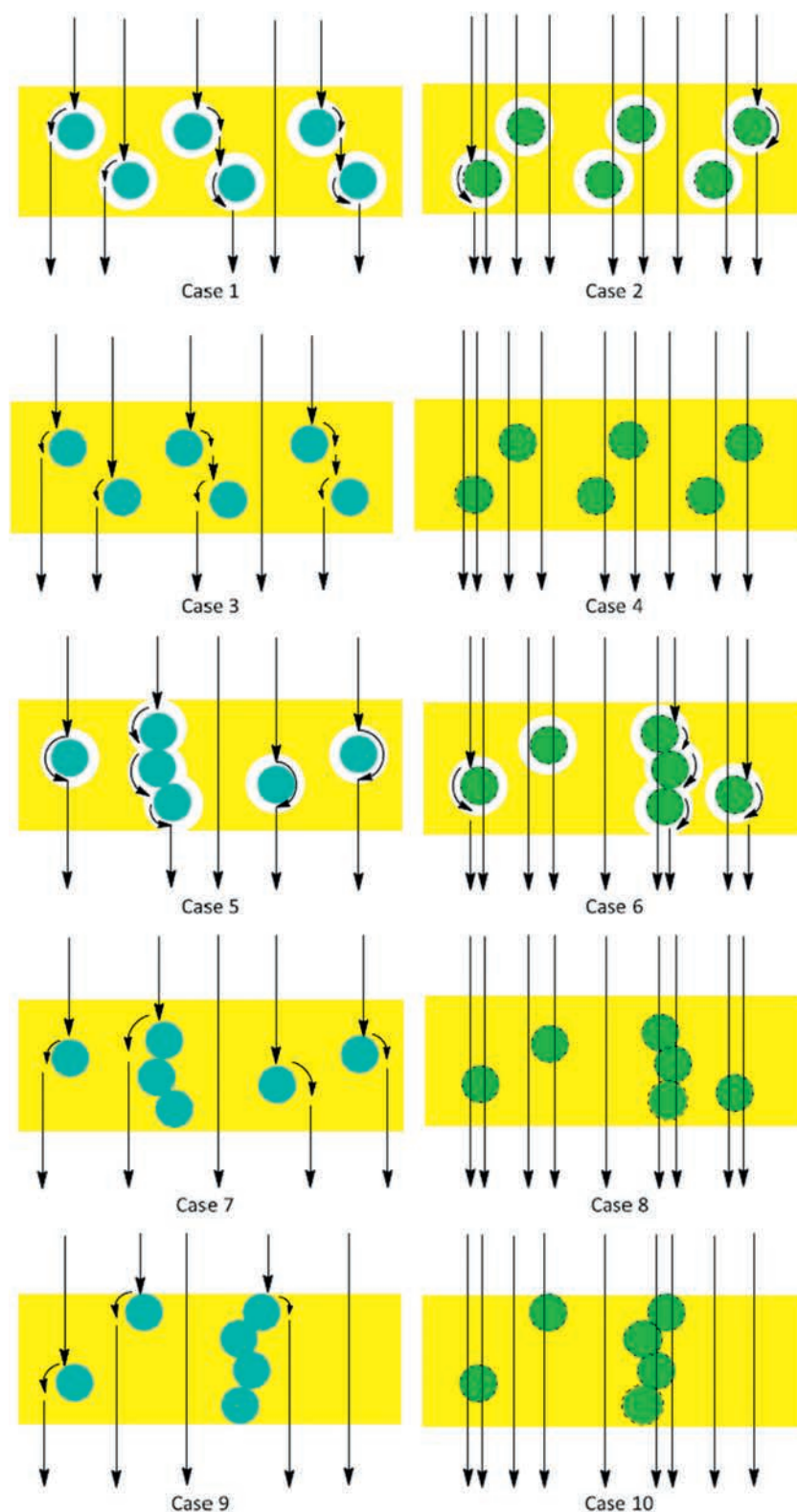


Fig. 2. Schematic diagram of separation layer structure of the MMMs and its corresponding gas transport pathway [75].

Amooghin *et al.* [77] also modified NaY by APDEMS, and embedded the modified particles into the Matrimid® 5218 matrix to prepare MMMs with defect free polymer/filler interface. Fig. 3 shows the grafting reaction between the APDEMS and zeolite surface, and also the proposed possible reaction between silane modified zeolite and Matrimid. As shown in Fig. 3, APDEMS reacts with the hydroxyl groups on zeolite surface, the amino group of APDEMS reacts with the imide group of Matrimid and

consequently forms the covalent bonding between zeolite and Matrimid, which results in the good interface compatibility between the two phases. Compared with pure Matrimid® membrane, the CO₂ permeability and CO₂/CH₄ selectivity of the MMMs with 15 wt% loading increased by 16% to $3.25 \times 10^{-15} \text{ mol} \cdot \text{m}^{-2} \cdot \text{s}^{-1} \cdot \text{Pa}^{-1}$ and by 57% to 57.1, respectively. Laghaei *et al.* [78] modified the surface of MCM-41 by 3-aminopropyltrimethoxysilane (APTMS) and trimethylchlorosilane

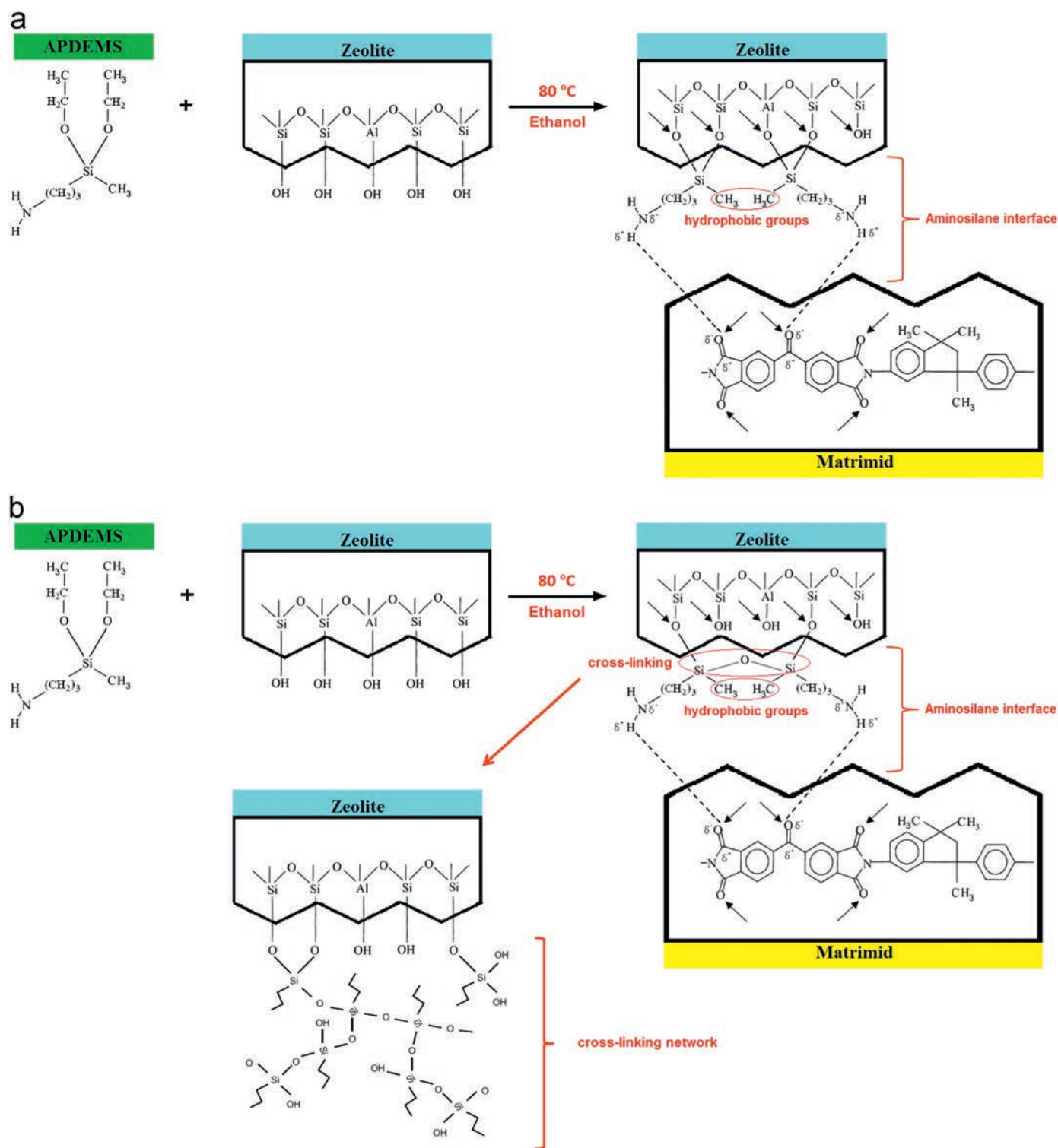


Fig. 3. The grafting reaction between APDEMS and zeolite surface, and also the reaction between Matrimid and the surface modified zeolite [77].

(TMCS). The APTMS-modified MCM-41 with polar N-H groups and long side chains had a good compatibility with PES matrix, which facilitated the preparation of defect free membranes with gas separation performance by 250% and 40% increment in CO₂ permeability and CO₂/CH₄ selectivity, respectively. However, the TMCS did not interact with the PES as strong as APTMS. Dong *et al.* [79] developed novel MMMs by establishing montmorillonite (MMT) functionalized with PEG and aminosilane coupling agents in a Pebax membrane. There were no evident interfacial voids in all MMMs, and the prepared

MMM with 40 wt% of MMT-HD702-PEG5000 displayed a CO₂ permeability of $1.50 \times 10^{-13} \text{ mol} \cdot \text{m} \cdot \text{m}^{-2} \cdot \text{s}^{-1} \cdot \text{Pa}^{-1}$ and a CO₂/N₂ selectivity of 70.73.

4.2. Grignard treatment

The Grignard treatment method can modify the filler surface, reduce the solvent–filler interaction, and recuperate the interfacial adhesion between filler and polymer. The Grignard treatment involves growing

Mg(OH)₂ whiskers on the filler surface, and consists of two steps: (i) a crystal seeding step and (ii) the crystal growth step. The Grignard treatment method creates roughened surface morphologies composed of whisker- and platelet-shaped nanocrystals, and the highly roughened filler surfaces are thought to promote adhesion at the polymer particle interface via thermodynamically-induced adsorption and physical entanglement of polymer chains in the whisker structures by minimizing the entropy penalty [46].

Zornoza *et al.* [80] prepared MMMs by adding ordered mesoporous silica MCM-41 spheres (MSSs), Grignard surface functionalized MSSs (Mg-MSSs) and hollow zeolite spheres into 6FDA-DAM polymer matrix. Because the polymer chain tends to be adsorbed onto the heterogeneous surface compared with the flat surface, once embedded in the 6FDA-DAM polymer matrix, Mg-MSSs external whisker-like structure promoted interfacial filler-polymer contact, which resulted in excellent adhesion between filler and polymer as shown in Fig. 4. The 6FDA-DAM-Mg-MSS MMM had the best performance with CO₂/N₂ and CO₂/CH₄ separation selectivities of 24.4 ($4.07 \times 10^{-13} \text{ mol} \cdot \text{m} \cdot \text{m}^{-2} \cdot \text{s}^{-1} \cdot \text{Pa}^{-1}$ of CO₂), and 31.5 ($4.17 \times 10^{-13} \text{ mol} \cdot \text{m} \cdot \text{m}^{-2} \cdot \text{s}^{-1} \cdot \text{Pa}^{-1}$ of CO₂), respectively.

4.3. Incorporation of additive

Expect polymer and inorganic filler, the addition of the third component as additive can improve compatibility between filler and polymer matrix. Such additives include PEG, ionic liquid (IL), and polyethylenimine (PEI).

PEG as a low molecular weight CO₂ selective agent can eliminate interfacial voids between the polymer chains and zeolite surface. Loloei *et al.* [81] investigated the effect of low molecular weight PEG 200 on the gas separation properties of Matrimid® 5218-ZSM-5 MMM, and demonstrated that there is a good compatibility between ZSM-5 and polymers.

Free ILs act like lubricants between the fillers and the polymer matrices, leading to good compatibility in the three-component MMMs and high CO₂ permeability of the MMMs. Hudiono *et al.* [82,83] demonstrated that ILs could behave like a wetting agent in polymer-zeolite MMMs and improve the compatibility between polymer and zeolite. Hao *et al.* [84] fabricated poly(ionic liquid)-IL-ZIF-8 MMMs and

demonstrated that the addition of ZIF-8 considerably improved gas permeability without compromising CO₂/N₂ and CO₂/CH₄ selectivities, indicating the absence of defects in the MMMs. Casado-Coterillo *et al.* [85] incorporated nanometer-sized ZIF-8 or HKUST-1 particles into the mixture of [emim][Ac] IL and chitosan (Cs) to fabricate MMMs and the Cs-IL-ZIF-8 MMMs had a maximum CO₂ permeability of over $1.68 \times 10^{-12} \text{ mol} \cdot \text{m} \cdot \text{m}^{-2} \cdot \text{s}^{-1} \cdot \text{Pa}^{-1}$.

Confined ILs can not only improve compatibility between the fillers and the polymer matrices, but also improve the CO₂ selectivity of the resulting MMMs further. Li *et al.* [86] incorporated a room temperature ionic liquid (IL) [bmim][Tf2N] into ZIF-8 cages, and then added the IL-incorporated ZIF-8 (IL@ZIF-8) into Pebax to prepare the Pebax-IL@ZIF-8 MMMs with toughened MOF-polymer interface. A mechanism of the formation of filler-polymer interfaces was proposed in Fig. 5. At the beginning of the membrane preparation, the PA blocks would assemble preferentially around the hydrophobic sites of IL@ZIF-8 particles owing to their hydrophobic-hydrophobic interaction. As the membrane had become nearly solidified, the solvent diffused out of the ZIF-8 framework and dragged the IL to the interfaces between fillers and polymers. Because the bulkier IL clusters have good compatibility with the polymer, the bulkier IL clusters embedded in the apertures of ZIF-8 could act as cross-linking agents between the two phases. Due to a stiffer interphase between the filler and the polymer and a reduction in the effective aperture size of ZIF-8, the Pebax-IL@ZIF-8 membranes displayed improved molecular sieving properties. Compared with pure Pebax membrane, CO₂ permeability, CO₂/N₂ selectivity and CO₂/CH₄ selectivity of the MMM with 15 wt% IL@ZIF-8 increased by 45%, 74% and 92%, respectively.

MIL-101(Cr) with a particle size of ~550 nm was chemically decorated with PEI rich in amine groups via a facile vacuum-assisted method, and the obtained PEI@MIL-101(Cr) was then incorporated into SPEEK to fabricate SPEEK-PEI@MIL-101(Cr) membranes [87]. Owing to the electrostatic interaction and hydrogen bond between sulfonic acid group and PEI, the PEI both in the pore channels and on the surface of MIL-101(Cr) improved the filler-polymer interface compatibility, and simultaneously rendered abundant amine carriers to facilitate the transport of CO₂ through reversible reaction. The SPEEK-PEI@MIL-101(Cr) membrane with 40 wt% PEI@MIL-101(Cr) displayed the highest ideal selectivities for CO₂/CH₄ and CO₂/N₂ which were 71.8 and 80.0, respectively,

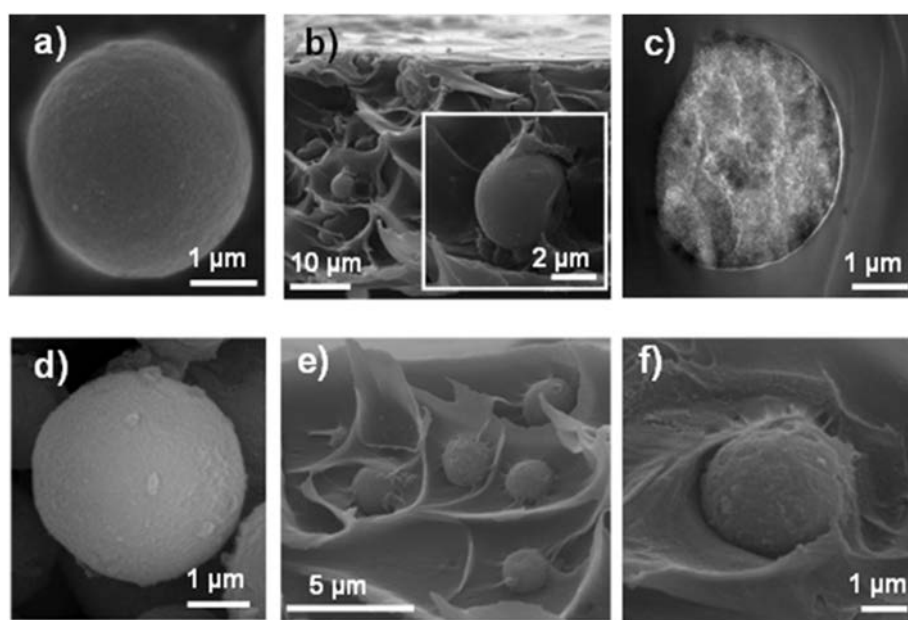


Fig. 4. SEM images based of: (a–c) MSSs [(a) individual particle, (b) 8 wt% MSS/6FDA:DAM MMM, and (c) TEM image of an embedded particle], and (d–f) Mg-MSSs [(d) individual particle, (e) 8 wt% Mg-MSS/6FDA:DAM MMM, and (f) inset of (e)] [80].

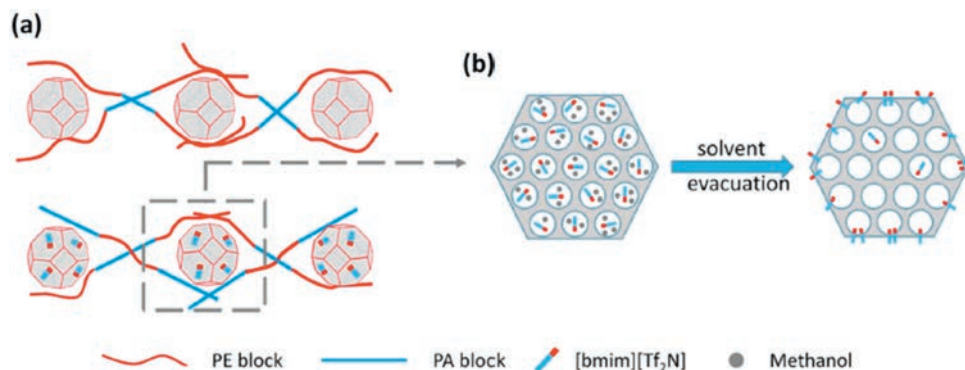


Fig. 5. Hypothetical mechanism of the toughening of filler-polymer interface: (a) the preferential adsorption of PA block on IL@ZIF-8 and (b) the aggregation of [bmim][Tf₂N] at the filler-polymer interface [86].

with a CO₂ permeability of $8.34 \times 10^{-13} \text{ mol} \cdot \text{m} \cdot \text{m}^{-2} \cdot \text{s}^{-1} \cdot \text{Pa}^{-1}$ at 0.1 MPa and 25 °C, which surpassed Robeson's upper bound revised in 2008.

4.4. Grafting

Inorganic nanofiller is modified by grafting with low molecular weight polymer containing EO and amine groups. Hydrogen bonding can be easier to form between polymer and modified inorganic nanofiller, which can enhance compatibility.

Li *et al.* [88] prepared MMMs by incorporating polyethyleneglycol- and polyethylenimine-functionalized graphene oxide nano-sheets (PEG-PEI-GO) into a commercial low-cost Pebax matrix. As shown in Fig. 6, GO was modified by grafting with PEI and PEG to fabricate PEG-PEI-GO nanosheets. Hydrogen bonding could form not only between the amino group of PEI and the ether oxygen group (or amide

group) of Pebax, but also between the ether oxygen group of PEG and amide group of Pebax. Hence, PEG and PEI on the surface of GO improved the interface compatibility between the Pebax matrix and GO nanosheets. The MMM with 10 wt% PEG-PEI-GO showed optimal gas separation performance with a CO₂ permeability of $4.46 \times 10^{-13} \text{ mol} \cdot \text{m} \cdot \text{m}^{-2} \cdot \text{s}^{-1} \cdot \text{Pa}^{-1}$, a CO₂/CH₄ selectivity of 45, and a CO₂/N₂ selectivity of 120, which surpassed Robeson's upper bound revised in 2008.

4.5. In situ polymerization

The added fillers participate in the polymer synthesis, which is called as *in situ* polymerization. The chemical bonding can form between polymer and filler by *in situ* polymerization, which is beneficial to improving compatibility.

[Cd₂L(H₂O)]₂ · 5H₂O (Cd-6F) synthesized using 6FDA as an organic ligand was introduced into the 6FDA-ODA polyimide matrix to achieve novel MOF MMMs [89]. As shown in Fig. 7, a specific interaction between the uncoordinated —COO[−]— on the surface of Cd-6F and the —NH₂ groups of the ODA monomer at the terminal of poly(6FDA-ODA) chains was introduced during the *in situ* polymerization. Compared with the pure 6FDA-ODA polyimide membrane, the as-prepared MMM displayed both higher permeability and selectivity due to the good polymer-MOFs compatibility resulted from the targeted interfacial interaction. The MMM exhibited a CO₂ permeability of $1.27 \times 10^{-14} \text{ mol} \cdot \text{m} \cdot \text{m}^{-2} \cdot \text{s}^{-1} \cdot \text{Pa}^{-1}$ with a CO₂/N₂ selectivity of 35.1, and CO₂/CH₄ selectivity of 44.8.

4.6. Polydopamine coating

Polydopamine (PD) is a good adhesion agent. PD can conveniently deposit and further adhere on virtually all types of inorganic and organic supports with controllable film thickness and durable stability *via* the oxidative self-polymerization of dopamine (DOP) in a mildly alkaline environment.

The nanosized ZIF-8 was coated by an ultrathin PD layer, and then incorporated into intrinsically microporous polyimide named TBDA2-6FDA-PI with Tröger's Base to prepare ZIF-8@PD-PI membrane [90]. The formation of hydrogen bond interaction between the abundant secondary or primary amine groups on PD molecules and the tertiary amine in TB-based PI polymers is beneficial to the improvement of compatibility between the two polymers as schematically shown in Fig. 8. For CO₂/N₂ (50/50, v:v) mixed gas, ZIF-8@PD-PI (20%) membrane exhibited a CO₂ permeability of $2.33 \times 10^{-13} \text{ mol} \cdot \text{m} \cdot \text{m}^{-2} \cdot \text{s}^{-1} \cdot \text{Pa}^{-1}$ and a CO₂/N₂ selectivity of 21 at 0.1 MPa. For CO₂/CH₄ (50/50, v:v) mixed gas, ZIF-8@PD-PI (20%) membrane exhibited a CO₂ permeability of $2.11 \times 10^{-13} \text{ mol} \cdot \text{m} \cdot \text{m}^{-2} \cdot \text{s}^{-1} \cdot \text{Pa}^{-1}$ and a CO₂/CH₄ selectivity of 27 at 0.1 MPa.

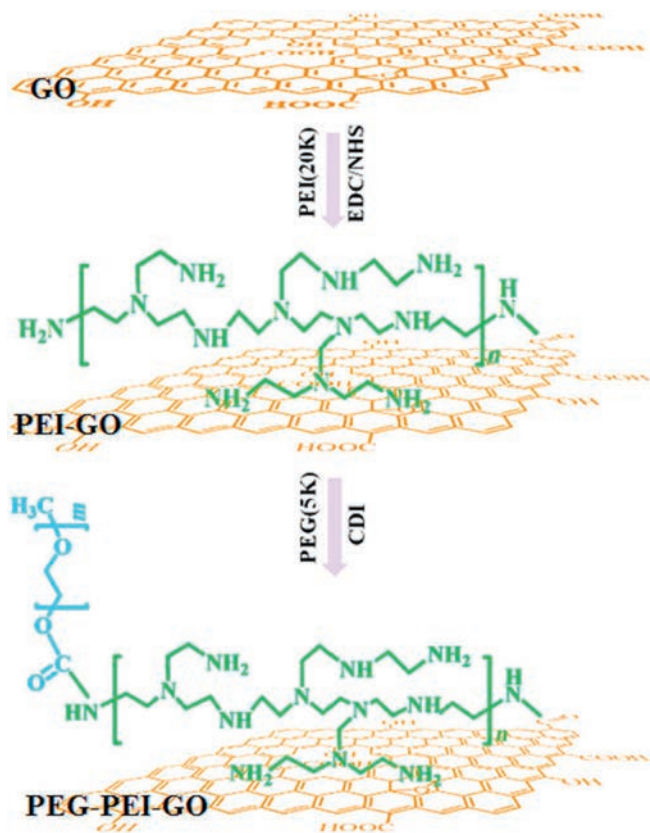


Fig. 6. Illustration of the preparation of PEG-PEI-GO [88].

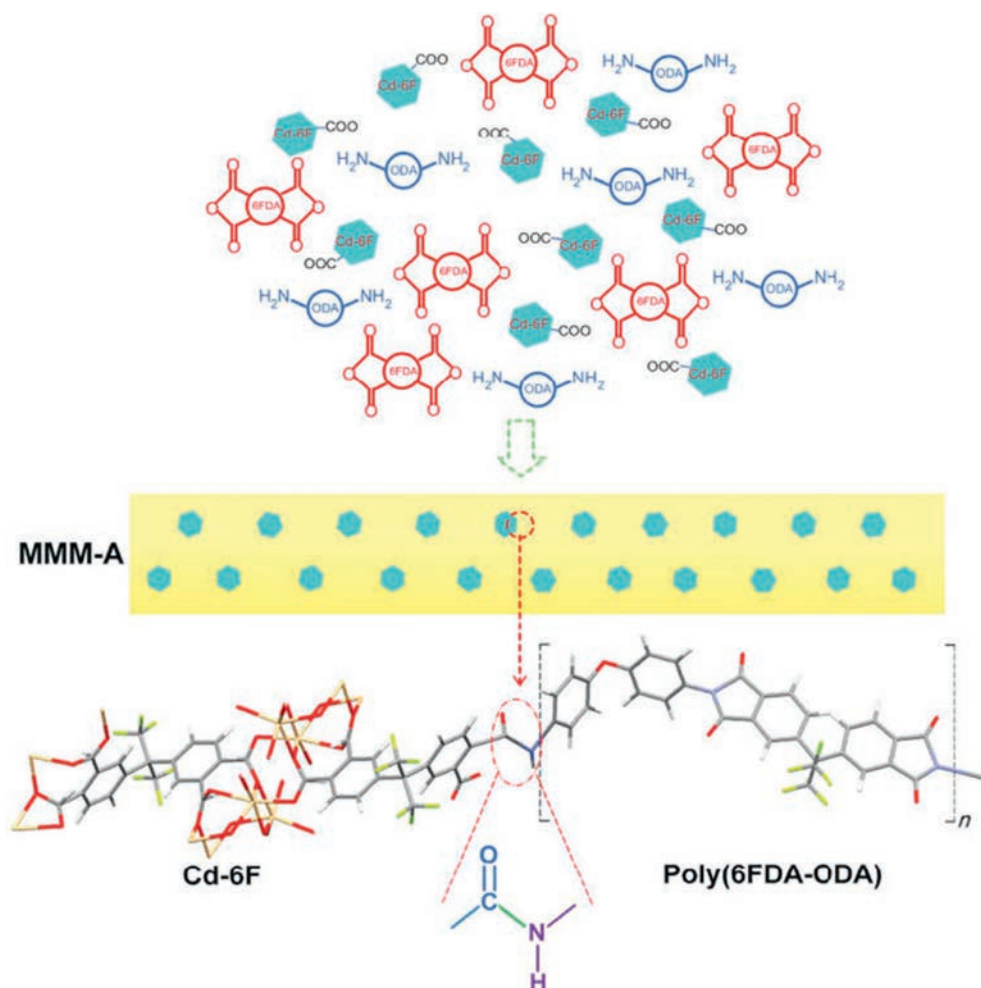


Fig. 7. Diagram of designed interaction between Cd-6F and 6FDA-ODA in MMM [89].

4.7. Particle fusion approach

Particle fusion method is very versatile, and can enhance compatibility between filler and polymer matrix.

Shahid *et al.* [91] prepared MOF based MMM with better compatibility via a particle fusion approach. Matrimid® polymer particles were first prepared by precipitating a Matrimid® polymer solution in water. The surface of these particles was then modified by the introduction

of imidazole groups as shown in Fig. 9(a). ZIF-8 nanoparticles were then grown *in-situ* to this modified polymer particle suspension by addition of the precursor for ZIF-8 synthesis. The resulted suspension was cast to dryness and annealed in a solvent-vapor environment to induce particle fusion, forming a dense MMM as shown in Fig. 9(b). The pendent imidazole units lead to a better compatibility between the polymer phase and the ZIF-8 nanoparticles. The excellent ZIF-8-polymer interfacial adhesion resulted in a significant improvement

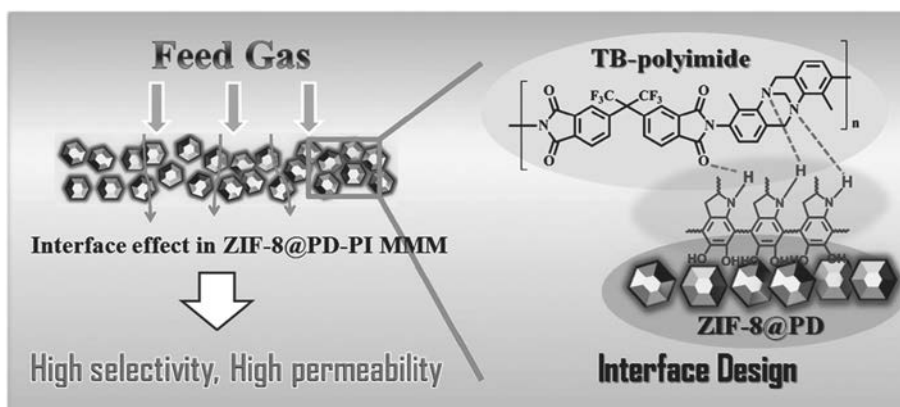


Fig. 8. Schematic illustration for interface design of ZIF-8@PD-PI membrane [90].

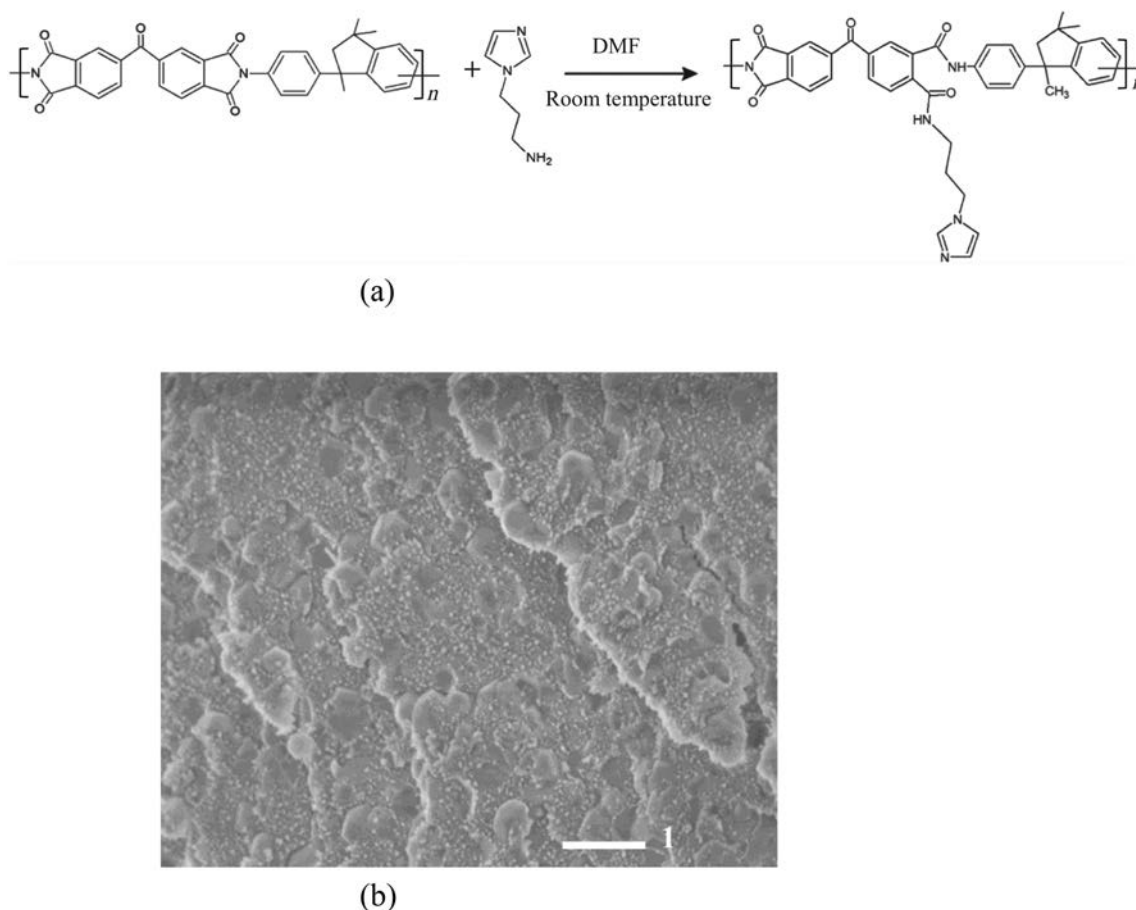


Fig. 9. Modification process of Matrimid® polymer particles (a) and SEM image of MMM containing 30 wt% ZIF-8 prepared by particle fusion (b) [91].

in both CO₂ permeability and CO₂/CH₄ selectivity. Compared with unfilled Matrimid®, the CO₂ permeability of the MMMs increased by 200% and the CO₂/CH₄ selectivity increased by 65%.

4.8. Polymer functionalization

Functionalized polymer is used to improve compatibility, which is called as polymer functionalization. Functionalized polymer can interact with functional groups containing filler, which lead to the enhanced compatibility.

Tien-Binh *et al.* [92] synthesized hydroxyl-functionalized homo- and co-polyimides 6FDA-(DAM)_x-(HAB)_y (with x:y molar ratio of 1:0; 2:1; 1:1; 1:2) and two MOFs [MIL-53(Al) and NH₂-MIL-53(Al)] to prepare MMMs. A strong interaction existed between the hydroxyl groups in the copolyimides and the amine groups in NH₂-MIL-53(Al), which enhanced polymer-filler compatibility. The MMM prepared with 6FDA-DAM-HAB (1:1) copolyimide and 10 wt% NH₂-MIL-53(Al) displayed a permeability/selectivity behavior approaching the 2008 Robeson's upper bound.

In brief, during modification process by using these methods except Grignard treatment, hydrogen bonding or chemical bonding forms, which leads to the fact that the interactions between polymer matrix and inorganic nanofiller improve interface compatibility.

5. Mixed Matrix Composite Membrane

So far, most mixed matrix membranes for CO₂ separation are free-standing membranes without porous membrane as a support layer. The thicknesses of these membranes range from several dozen to several hundred micrometers. However, industrial demands on the

membranes of higher productivity motivate researchers to fabricate integrally skinned asymmetric membranes or composite membranes. Hence, mixed matrix asymmetric membranes and mixed matrix composite membranes are developed. The mixed matrix composite membranes are reviewed in the section. A mixed matrix composite membrane consists of a thin separation layer and a support layer, and the thin separation layer known as mixed matrix layer is deposited on the asymmetric support layer. The separation layer is ultrathin, and has only several micrometers at most. When there is a poor compatibility between polymer and filler, interface voids are easier to be formed in the separation layer. For the mixed matrix composite membrane, how to avoid voids is a challenging subject. Recently, mixed matrix composite membranes have attracted the great attention. Most researches have focused on the forms of hollow fiber and flat mixed matrix composite membranes.

5.1. Hollow fiber mixed matrix composite membrane

Ekiner and Kulkarni [93] reported a patent on the hollow fiber mixed matrix composite membranes in 2003. Later, Chung's group does a lot of researches on the hollow fiber mixed matrix composite membranes [94–98]. The outer diameter of these membranes ranges from ~650 to ~1000 μm, the inner diameter ranges from ~350 to ~600 μm, and the thickness of the dense selective layer ranges from 0.15 to 12 μm.

The hollow fiber mixed matrix composite membranes [94–97] are spun by the co-extrusion technique using a dual-layer spinneret as depicted in relative literatures [99]. The flow rates of the bore fluid and both dope solutions are controlled by three pumps. The as-spun hollow fibers are rinsed in the clean water bath for several days to remove the remaining solvent and then carried out solvent exchange

without further drying. Finally, these fibers are dried in the air at ambient temperature for use. By lowering the outer layer flow rate (while keeping other spinning conditions constant), the thickness of the outer layer can be reduced [95]. To avoid voids, they attempt several posttreatment methods such as heat treatment and two-step coating, and *p*-xylenediamine/methanol soaking. Li *et al.* [96] employed heat treatment and two-step coating processes to bring out the separation properties of zeolite beta imbedded in the polymer matrix for defect-free PES–zeolite beta/P84 hollow fiber membrane. Compared with that of neat PES dense films, the CO₂/CH₄ selectivity of the hollow fiber membranes increased by around 10%–20%. Jiang *et al.* [97] adopted a novel *p*-xylenediamine/methanol soaking method to efficiently remove the PSf–zeolite interface defects of the PSf–zeolite beta/Matrimid® hollow fiber membranes, and found that CO₂/CH₄ ideal selectivities of the PSf–zeolite beta/Matrimid® hollow fiber membranes roughly increased by 50% in comparison with that of the neat PSf/Matrimid® hollow fiber membrane. Hydrogen bonding was proposed as the possible mechanism for the tighter attachment between the PSf matrix and filler (Fig. 10). In addition, Chen *et al.* [98] developed novel hollow fiber membranes by surface coating ultrathin layers of a PEG containing hybrid material onto the asymmetric PES hollow fiber substrate. The fabricated membranes exhibited an impressive CO₂/N₂ selectivity of 50 with the CO₂ permeance of $1.01 \times 10^{-8} \text{ mol} \cdot \text{m}^{-2} \cdot \text{s}^{-1} \cdot \text{Pa}^{-1}$ at 25 °C and 0.2 MPa.

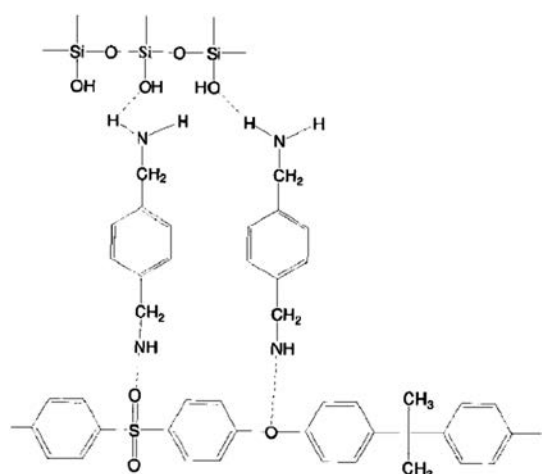


Fig. 10. Mechanism of *p*-xylenediamine priming and possible structure [97].

5.2. Flat mixed matrix composite membrane

Kulprathipanja and Charoenphol [100] published a patent on mixed matrix membrane for separation of gases in 2004. In the patent, a mixed matrix composite membrane comprised PEG, silicone rubber and activated carbon on a porous support. The membrane preferably also comprised a carbonate such as potassium carbonate. Later, Kulprathipanja *et al.* [101] published another patent. In that patent, a mixed matrix composite membrane comprised a nitrogen containing compound such as amine, silicone rubber and activated carbon on a porous support. The membrane might also comprise a plasticizer such as PEG. Thereafter, a lot of academic papers on flat mixed matrix composite membranes are published.

5.2.1. Poly(dimethylsiloxane) based mixed matrix composite membrane

Some researchers select rubbery poly(dimethylsiloxane) (PDMS) as polymer matrix. de Clippel *et al.* [102], developed a defect-free mixed matrix composite membrane by filling a PDMS top layer with porous carbon–silica microspheres on a polyimide (PI)/polypropylene (PP) membrane, and the derived MMM displayed a CO₂ permeance of 2.81

$\times 10^{-8} \text{ mol} \cdot \text{m}^{-2} \cdot \text{s}^{-1} \cdot \text{Pa}^{-1}$, and a CO₂/H₂ selectivity of 4.7 at 1.0 MPa and 25 °C. Wang *et al.* [103] also incorporated mesoporous KIT-6 modified by phenyltriethoxysilane (PTES) into PVDF supported PDMS to fabricate PDMS–p-KIT-6/PVDF membranes, but the CO₂/N₂ ideal selectivity of the membrane was too low.

5.2.2. PIM-1 based mixed matrix composite membrane

Some researchers choose glassy PIM-1 as polymer matrix. Khan *et al.* [104] coated the mixture of PIM-1 and multiwalled carbon nanotubes (MWCNTs) functionalized with PEG on microporous polyacrylonitrile (PAN) membrane to fabricate the PIM-1–f-MWCNT/PAN membrane. The derived MMM with f-MWCNT loading of 2 wt% reached a high CO₂ permeance of $3.68 \times 10^{-6} \text{ mol} \cdot \text{m}^{-2} \cdot \text{s}^{-1} \cdot \text{Pa}^{-1}$, and a CO₂/N₂ ideal selectivity of 33.5 at 0.2 MPa and 27 °C.

5.2.3. EO containing polymer based mixed matrix composite membrane

Because Pebax 1657 is a commercial candidate polymer material containing EO groups for CO₂ separation, it is also used as polymer matrix. Solid nanoparticles, two-dimensional materials, and three-dimensional porous material are selected as nanofillers, respectively. When solid TiO₂ was chosen as nanofillers, defect-free Pebax 1657–TiO₂/PVC membranes with TiO₂ loading of 3 wt% showed the best performance [105]. Shen *et al.* [106] used the mixture of Pebax 1657 and MoS₂ nanosheets as the selective layer, PDMS as the gutter layer, and PSf as a support substrate to prepare the mixed matrix composite membrane. The prepared membrane with 0.15 wt% MoS₂ nanosheets exhibited the best performance with a CO₂ permeance of $5.80 \times 10^{-9} \text{ mol} \cdot \text{m}^{-2} \cdot \text{s}^{-1} \cdot \text{Pa}^{-1}$, and CO₂/N₂ ideal selectivity of 93 at 0.2 MPa and 30 °C. Zarshenas *et al.* [107] fabricated mixed matrix membranes by incorporating nano-zeolite NaX into Pebax 1657 as a separation layer on the PES membrane as a support layer. The membrane containing 2 wt% zeolite NaX showed a CO₂ permeance of $7.87 \times 10^{-10} \text{ mol} \cdot \text{m}^{-2} \cdot \text{s}^{-1} \cdot \text{Pa}^{-1}$ and a CO₂/N₂ ideal selectivity of 121.5 at 0.7 MPa and 25 °C. Li *et al.* [108] deposited the mixture of Pebax 1657 and ZIF-7 on a porous PAN support to prepare Pebax 1657–ZIF-7/PAN membranes with polytrimethylsilylpropyne (PTMSP) gutter layer. The Pebax 1657–ZIF-7/PAN membrane with 22 wt% ZIF-7 displayed a CO₂ permeance of $4.59 \times 10^{-8} \text{ mol} \cdot \text{m}^{-2} \cdot \text{s}^{-1} \cdot \text{Pa}^{-1}$, and CO₂/N₂ ideal selectivity and CO₂/CH₄ ideal selectivity of 97 and 30, respectively at 0.375 MPa and 25 °C. Jomekian *et al.* [109] coated Pebax 1657–ZIF-8 on PES layer to fabricate Pebax 1657–ZIF-8/PES membrane. The as-prepared membrane showed a CO₂ permeance of $1.21 \times 10^{-7} \text{ mol} \cdot \text{m}^{-2} \cdot \text{s}^{-1} \cdot \text{Pa}^{-1}$, and a CO₂/N₂ ideal selectivity of 16.1 at 0.8 MPa.

In addition, PEG is also an important polymer material containing EO groups. Iron dopamine nanoparticles (FeDA NPs) were incorporated into a nanoscale thick PEG matrix on a highly permeable PDMS prelayer spin-coated onto a porous PAN substrate to form mixed matrix composite membranes [110]. The as-prepared membrane displayed excellent gas separation performance with a CO₂ permeance of $\sim 4.02 \times 10^{-7} \text{ mol} \cdot \text{m}^{-2} \cdot \text{s}^{-1} \cdot \text{Pa}^{-1}$ and an enhanced CO₂/N₂ ideal selectivity of over 35 at 0.1 MPa and 35 °C.

5.2.4. Facilitated transport based mixed matrix composite membrane

Facilitated transport based mixed matrix composite membranes have also been investigated. They are roughly reviewed in the lasted two reviews [10,111]. In this section, they are discussed in detail according to types of polymer matrix.

Our group carried out lots of researches on flat mixed matrix composite membranes, and examined structure–property relationship. Generally, our group chose amine containing polymer as polymer matrix to prepare different flat mixed matrix composite membranes by the addition of different nanofillers. Firstly, our group selected the conventional nanomaterials as nanofillers. Yu *et al.* [112] fabricated the mixed matrix composite membranes by incorporating CO₂-selective adsorptive LUDOX® silica nanoparticles *in situ* into the tertiary

amine containing polyamide membrane formed by interfacial polymerization. The membrane displayed a CO_2 permeance of $1.99 \times 10^{-8} \text{ mol} \cdot \text{m}^{-2} \cdot \text{s}^{-1} \cdot \text{Pa}^{-1}$ and a CO_2/N_2 selectivity of 85.4 at 0.1 MPa. Wang *et al.* [75] found that surface modification of pristine inorganic nanofillers (MWCNT, SiO_2 and ZSM-5) endowed with amine groups could eliminate or reduce interface voids and improve the interface compatibility between PVAm polymer chains and modified inorganic nanofillers.

Based on this, silane coupling agents are used to couple polymer with layer nanomaterials in order to eliminate or remove interface voids. At the same time, layer nanomaterials are beneficial to CO_2 facilitated transport. Liao *et al.* [113] synthesized the polyethylenimine-based copolymer PEIE with abundant amine groups and moderate hydroxyl groups, chose PEIE as a polymer matrix, chose nanosized hydrocalcite (HT) as a filler, used 3-aminopropyltriethoxysilane (APTES) as a molecular bridge to couple the PEIE and HT, and then coated the PEIE-HT complex on PSf membrane to fabricate the PEIE-HT/PSf membrane. In view of the mobile carriers within the interlayer gap of HT, high-speed CO_2 transport channels were successfully constructed, and the PEIE-HT/PSf membrane exhibited a high CO_2 permeance up to $1.91 \times 10^{-6} \text{ mol} \cdot \text{m}^{-2} \cdot \text{s}^{-1} \cdot \text{Pa}^{-1}$ and a CO_2/N_2 selectivity of 268 at 0.11 MPa. To verify high-speed CO_2 transport channels of HT further, Liao *et al.* [43] chose PVAm and HT as a polymer matrix and filler, respectively, used 3-Glycidyloxypropyltrimethoxysilane (GLYMO) as a molecular bridge to couple the PVAm and HT, and then prepared the PVAm-HT/PSf membrane. The PVAm-HT/PSf membrane exhibited a high CO_2 permeance of $1.07 \times 10^{-6} \text{ mol} \cdot \text{m}^{-2} \cdot \text{s}^{-1} \cdot \text{Pa}^{-1}$ and a CO_2/N_2 selectivity of 296 at 0.11 MPa. To evaluate the effect of arrangement of layer nanomaterials on gas permselectivity, Qiao *et al.* [114] immobilized montmorillonite layers bonded and aligned with the chain stretching orientation of polyvinylamineacid onto a porous PSf substrate to fabricate aligned montmorillonite/polysulfone (AMT/PSf) membranes. Owing to aligned interlayer gaps as high-speed CO_2 transport channels, the AMT/PSf membrane achieved a high CO_2 permeance of about $2.68 \times 10^{-7} \text{ mol} \cdot \text{m}^{-2} \cdot \text{s}^{-1} \cdot \text{Pa}^{-1}$ and a high mixed-gas selectivity for CO_2 .

Apart from the common nanomaterials and layered nanomaterials, MOF and covalent organic framework (COF) are also used as nanofillers, respectively. On the one hand, the addition of MOF and COF disturbs polymer chain packing, and increases free volume, which results in the improvement of CO_2 permeance. On the other hand, CO_2 molecules can transport through the pore of MOF and COF. Zhao *et al.* [42] incorporated ZIF-8 into a PVAm solution, and coated the PVAm-ZIF-8 mixture on a PSf support membrane to prepare the PVAm-ZIF-8/PSf membrane. Compared with the PVAm/PSf membrane, the CO_2 permeance and CO_2/N_2 selectivity of the PVAm-ZIF-8/PSf membrane with 13.1 wt% ZIF-8 increased by about 325% and 65% at 0.15 MPa and 79% and 140% at 2.0 MPa, respectively. However, owing to the nonselective voids between aggregated nanoparticles, CO_2/N_2 selectivity of the PVAm-ZIF-8/PSf membrane with 23.1 wt% ZIF-8 decreased to a lower value than that of the PVAm/PSf membrane at a feed pressure of over 1.0 MPa. Cao *et al.* [115] incorporated a highly compatible covalent organic framework COF-LZU1 into PVAm to fabricate the PVAm-COF/PSf membranes. The PVAm-COF/PSf membrane with 10 wt% COF-LZU1 exhibited a CO_2 permeance of $1.33 \times 10^{-7} \text{ mol} \cdot \text{m}^{-2} \cdot \text{s}^{-1} \cdot \text{Pa}^{-1}$ and a CO_2/H_2 selectivity of 15 at 0.15 MPa.

In addition, organic nanoparticles are also chosen as nanofillers. Zhao *et al.* [68] coated blend of polyaniline (PANI) nanoparticles and PVAm on PSf membranes to prepare the PVAm-PANI/PSf membranes. At CO_2 partial pressure of 0.02 MPa, the PVAm-PANI/PSf membrane with 17 wt% PANI nanosheets showed a CO_2 permeance of $4.02 \times 10^{-7} \text{ mol} \cdot \text{m}^{-2} \cdot \text{s}^{-1} \cdot \text{Pa}^{-1}$ and a CO_2/N_2 selectivity of 120. To prevent the agglomeration of PANI nanomaterials and improve the interface compatibility between PVAm and PANI nanofillers, PANI nanorods modified by poly(vinylpyrrolidone) (PVP) adsorption layer were incorporated into PVAm matrix to fabricate the PVAm-PANI/PSf

membranes [69]. The as-prepared PVAm-PANI/PSf membrane displayed a high CO_2 permeance of $1.03 \times 10^{-6} \text{ mol} \cdot \text{m}^{-2} \cdot \text{s}^{-1} \cdot \text{Pa}^{-1}$ and CO_2/N_2 selectivity of 240 at 0.11 MPa.

Besides our group, other researchers also use PVAm as polymer matrix. Deng and Hägg [116] incorporated 1 wt% CNTs into the polymer matrix of PVAm and polyvinyl alcohol (PVA), and prepared the PVAm-PVA-CNT/PSf membrane on PSf membrane by dip-coating method for high pressure gas transport measurements. At 1.0 and 1.5 MPa, the CO_2 permeance of the PVAm-PVA-CNT/PSf membrane was more than doubled in comparison with counterpart PVAm-PVA/PSf membrane. Shen *et al.* [117] added GO grafted with hyperbranched PEI (HPEI-GO) into the polymer matrix of PVAm and Cs on a porous PSf support to fabricate PVAm-Cs-HPEI-GO/PSf membrane. For CO_2/N_2 (10:90/v:v) mixed gas, the as-prepared membrane with 2.0 wt% HPEI-GO displayed a CO_2 permeance of $1.21 \times 10^{-8} \text{ mol} \cdot \text{m}^{-2} \cdot \text{s}^{-1} \cdot \text{Pa}^{-1}$ and a CO_2/N_2 ideal selectivity of 90. The as-prepared membrane with 3.0 wt% HPEI-GO displayed a CO_2 permeance of $1.05 \times 10^{-8} \text{ mol} \cdot \text{m}^{-2} \cdot \text{s}^{-1} \cdot \text{Pa}^{-1}$ and a CO_2/N_2 ideal selectivity of 107 at 0.1 MPa and 25 °C.

Ho's group incorporates different inorganic nanofillers into PVA matrix containing amine carriers to prepare facilitated transport mixed matrix composite membranes. Xing and Ho [118] incorporated fumed silica (FS), and the resulting membrane with 22.3 wt% FS loading displayed the best performance with a CO_2 permeance of $1.37 \times 10^{-8} \text{ mol} \cdot \text{m}^{-2} \cdot \text{s}^{-1} \cdot \text{Pa}^{-1}$ and a CO_2/H_2 selectivity of 87 at 1.52 MPa and 107 °C. Zhao *et al.* [119] incorporated MWCNTs, and the resulting membrane with 2 wt% MWCNTs showed a CO_2 permeance of $1.12 \times 10^{-8} \text{ mol} \cdot \text{m}^{-2} \cdot \text{s}^{-1} \cdot \text{Pa}^{-1}$ and a CO_2/H_2 selectivity of 43 at 1.52 MPa and 107 °C. The membrane performance was maintained without significant change for 444 h. To improve affinity with the hydrophilic membrane matrix, Ansaloni *et al.* [120] incorporated amino-functionalized multi-walled carbon nanotubes (AF-MWNTs). The resulting membrane with 2.3 wt% AF-MWNTs displayed a CO_2 permeance of $1.11 \times 10^{-8} \text{ mol} \cdot \text{m}^{-2} \cdot \text{s}^{-1} \cdot \text{Pa}^{-1}$, a CO_2/N_2 selectivity of 360, a CO_2/CH_4 selectivity of 277, and a CO_2/H_2 selectivity of 56 at 1.5 MPa and 107 °C. Moreover, the resulting membrane demonstrated a good stability.

For flat mixed matrix composite membranes, in addition to material design and selection, technology of membrane formation is very critical for obtaining good separation performance. The flat mixed matrix composite membrane can be mainly fabricated by solution casting method and interfacial polymerization. The solution casting method is simple and cheap. Hence, it is universally used. The mixture solution is cast on substrate (porous support membrane) with a pre-set wet coating thickness by a casting knife, then is dried under certain conditions. After the solvent evaporation, the flat mixed matrix composite membrane is fabricated successfully. To solve the problem of void creation between polymer and filler in conventional solution-casting methods for the formation of MMMs, casting solutions were prepared as follows [107]. A filler suspension was prepared by adding a specific amount of fillers to solvent and sonicating. Then, a quarter of the polymer solution was added to the filler suspension, stirred and sonicated. This procedure was continued until all of the polymer solution was added to the filler suspension and a homogenous casting solution was obtained.

Compared with solution casting method, interfacial polymerization is rather cockamamie and wastes a great amount of organic solvent. The flat mixed matrix composite membrane was fabricated by interfacial polymerization as follows [112]. The flat sheet support membrane was initially immersed into the aqueous phase for a certain time and then the excess solution was drained from the membrane surface. Subsequently, the impregnated membrane was placed into the organic phase for a certain time at a certain temperature. After that, the resulted composite membrane was rinsed with pure organic solvent and then heat-treated. Furthermore, the composite membrane was washed with deionized water to eliminate excess monomers and byproducts. Finally, the resulted membrane was kept under certain conditions. To solve the problem of void creation between polymer and filler, fillers

should be added to the aqueous phase or organic phase in which the fillers can be dispersed uniformly [112].

Generally speaking, compared with hollow fiber mixed matrix composite membrane, flat mixed matrix composite membrane possesses higher CO₂ permeance and higher CO₂/gas selectivity.

6. Future Direction

MMMs are a promising new generation of membranes for CO₂ separation. Compared with polymer membranes, CO₂ permeability and CO₂/gas selectivity of the MMMs both increase by the incorporation of suitable nanofillers. Therefore, in the future, MMMs are still the key research field to improve performance of polymer membranes. Some aspects on MMMs need to be explored further as follows:

- (1) Developing new polymers with high permeability and selectivity.
- (2) Synthesizing new nanofillers with suitable pore structure and particle size [9,121], especially organic nanofillers that have interaction with CO₂ molecules.
- (3) Investigating the relationship between interface morphology and gas transport property systematically and qualitatively.
- (4) Exploring new methods to improve compatibility between polymer and filler, and enhance gas permselectivity of the MMMs simultaneously.
- (5) Developing high performance mixed matrix composite membranes for industrial application.
- (6) Large pilot scale testing of membranes based on MMM approach [9].
- (7) Employing high performance mixed matrix composite membranes to prepare MMM modules for industrial application.
- (8) Establishing the membrane separation plant with MMM modules, which makes sure that membrane separation plant has advantages such as low cost and less energy consumption.

7. Conclusions

To improve CO₂ separation performance of polymer membranes, a large number of MMMs have been developed. Generally, MMMs contain two or more different components. Polymer matrix forms a continuous phase, and inorganic or organic fillers act as a dispersed phase. To prepare high performance MMMs for CO₂ separation, correct selection of polymer matrix and filler is essential. The polymer should possess high CO₂ permeability and high CO₂/gas selectivity. Moreover, the polymer should have high mechanical strength, and good thermal stability, chemical stability and processability. Matrimid® is the best polymer for CO₂/CH₄ separation under high pressure, and PVAm is the best polymer for CO₂/N₂, CO₂/CH₄ and CO₂/H₂ separation under low pressure. The filler should have high selectivity, good compatibility with polymer matrix, and small particle size. In the high performance MMMs, the fillers not only disturb polymer chain packing and increase free volume, but also facilitate CO₂ transport by itself. Compared with inorganic fillers, organic fillers are emerging fillers. PANI is the best filler for CO₂/N₂ separation, NHs is the best filler for CO₂/CH₄ separation, and MIL-53 is the best filler for CO₂/H₂ separation.

Owing to the differences between polymer matrix and filler, there are different interface morphologies between polymer matrix and filler. When there is poor compatibility between polymer matrix and filler, interface voids form. When the size of interface voids was larger than the mean free path of the gas molecules, and the interconnectivity of interface voids formed interface void channels across the MMMs, gas permeability increased and gas selectivity decreased with increasing feed pressure.

To avoid interface voids and improve membrane performance, researchers adopt eight methods including silane coupling, Grignard treatment, incorporation of additive, grafting, *in situ* polymerization, PD coating, particle fusion approach and polymer functionalization to

enhance interface compatibility. In principle, during modification process by using these methods except Grignard treatment, hydrogen bonding or chemical bonding forms, which leads to the fact that the interactions between polymer matrix and inorganic nanofiller improve interface compatibility.

To achieve higher productivity for industrial application, mixed matrix composite membranes are developed. Compared with hollow fiber mixed matrix composite membrane, flat mixed matrix composite membrane possesses higher CO₂ permeance and higher CO₂/gas selectivity.

In the future, further research on MMMs should be focused on the following aspects. On the one hand, researchers should develop new polymer and new filler to prepare high performance lab-scale MMMs, and investigate the effect of interface morphology on gas transport property. On the other hand, researchers should fabricate large-scale mixed matrix composite membranes with high permselectivity, and then assemble membrane modules to build membrane separation plant.

Nomenclature

A	membrane area, m ²
L_c	characteristic length of the core region, m
l	membrane thickness, m
P	permeability coefficient, mol·m·m ⁻² ·s ⁻¹ ·Pa ⁻¹
ΔP	transmembrane partial pressure, Pa
Q	permeation rate, m ³ (STP)·s ⁻¹
R	permeance, mol·m ⁻² ·s ⁻¹ ·Pa ⁻¹
x	the molar fraction of gas species in the feed side
y	the molar fraction of gas species in the permeate side
α_i/j	ideal gas selectivity
α_i/j	mixed gas selectivity or separation factor

Subscripts

i	gas species
j	gas species

References

- [1] P. Bernardo, E. Drioli, G. Golemme, Membrane gas separation: A review/state of the art, *Ind. Eng. Chem. Res.* 48 (2009) 4638–4663.
- [2] N. Du, H.B. Park, M.M. Dal-Cin, M.D. Guiver, Advances in high permeability polymeric membrane materials for CO₂ separations, *Energy Environ. Sci.* 5 (2012) 7306–7322.
- [3] D.F. Sanders, Z.P. Smith, R. Guo, L.M. Robeson, J.E. McGrath, D.R. Paul, B.D. Freeman, Energy-efficient polymeric gas separation membranes for a sustainable future: A review, *Polymer* 544 (2013) 729–4761.
- [4] L.M. Robeson, The upper bound revisited, *J. Membr. Sci.* 320 (2008) 390–400.
- [5] T.-S. Chung, L.Y. Jiang, Y. Li, S. Kulprathipanja, Mixed matrix membranes (MMMs) comprising organic polymers with dispersed inorganic fillers for gas separation, *Prog. Polym. Sci.* 32 (2007) 483–507.
- [6] H. Cong, M. Radosz, B. Towler, Y. Shen, Polymer-inorganic nanocomposite membranes for gas separation, *Sep. Purif. Technol.* 55 (2007) 281–291.
- [7] G. Dong, H. Li, V. Chen, Challenges and opportunities for mixed-matrix membranes for gas separation, *J. Mater. Chem. A* 1 (2013) 4610–4630.
- [8] R. Nasir, H. Mukhtar, Z. Man, D.F. Mohshim, Material advancements in fabrication of mixed-matrix membranes, *Chem. Eng. Technol.* 36 (2013) 717–727.
- [9] M. Rezakazemi, A. Ebadi Amooghin, M.M. Montazer-Rahmati, A.F. Ismail, T. Matsuura, State-of-the-art membrane based CO₂ separation using mixed matrix membranes (MMMs): An overview on current status and future directions, *Prog. Polym. Sci.* 39 (2014) 817–861.
- [10] Z. Tong, W.S.W. Ho, Facilitated transport membranes for CO₂ separation and capture, *Sep. Sci. Technol.* 52 (2017) 156–167.
- [11] S. Wang, X. Li, H. Wu, Z. Tian, Q. Xin, G. He, D. Peng, S. Chen, Y. Yin, Z. Jiang, M.D. Guiver, Advances in high permeability polymer-based membrane materials for CO₂ separations, *Energy Environ. Sci.* 9 (2016) 1863–1890.
- [12] Y. Li, T.-S. Chung, S. Kulprathipanja, Novel Ag⁺-zeolite/polymer mixed matrix membranes with a high CO₂/CH₄ selectivity, *AIChE J.* 53 (2007) 610–616.
- [13] C.-Y. Liang, P. Uchytel, R. Petrychkevych, Y.-C. Lai, K. Friess, M. Sipek, M. Mohan Reddy, S.-Y. Suen, A comparison on gas separation between PES (polyethersulfone)/MMT (Na-montmorillonite) and PES/TiO₂ mixed matrix membranes, *Sep. Purif. Technol.* 92 (2012) 57–63.
- [14] R. Nasir, H. Mukhtar, Z. Man, M.S. Shaharun, M.Z. Abu Bakar, Effect of fixed carbon molecular sieve (CMS) loading and various di-ethanolamine (DEA) concentrations on the performance of a mixed matrix membrane for CO₂/CH₄ separation, *RSC Adv.* 5 (2015) 60814–60822.

- [15] R. Nasir, H. Mukhtar, Z. Man, B.K. Dutta, M.S. Shaharun, M.Z. Abu Bakar, Mixed matrix membrane performance enhancement using alkanolamine solution, *J. Membr. Sci.* 483 (2015) 84–93.
- [16] D. Şen, H. Kalıpçılar, L. Yilmaz, Development of polycarbonate based zeolite 4A filled mixed matrix gas separation membranes, *J. Membr. Sci.* 303 (2007) 194–203.
- [17] R. Adams, C. Carson, J. Ward, R. Tannenbaum, W. Koros, Metal organic framework mixed matrix membranes for gas separations, *Microporous Mesoporous Mater.* 131 (2010) 13–20.
- [18] J. Ahmad, M.B. Hägg, Effect of zeolite preheat treatment and membrane post heat treatment on the performance of polyvinyl acetate/zeolite 4A mixed matrix membrane, *Sep. Purif. Technol.* 115 (2013) 163–171.
- [19] J. Ahmad, M.-B. Hägg, Preparation and characterization of polyvinyl acetate/zeolite 4A mixed matrix membrane for gas separation, *J. Membr. Sci.* 427 (2013) 73–84.
- [20] A.L. Khan, C. Klayson, A. Gahlaut, X. Li, I.F.J. Vankelecom, SPEEK and functionalized mesoporous MCM-41 mixed matrix membranes for CO₂ separations, *J. Mater. Chem.* 22 (2012) 20057–20064.
- [21] Q. Xin, T. Liu, Z. Li, S. Wang, Y. Li, Z. Li, J. Ouyang, Z. Jiang, H. Wu, Mixed matrix membranes composed of sulfonated poly(ether ether ketone) and a sulfonated metal-organic framework for gas separation, *J. Membr. Sci.* 488 (2015) 67–78.
- [22] L. Ge, W. Zhou, V. Rudolph, Z. Zhu, Mixed matrix membranes incorporated with size-reduced Cu-BTC for improved gas separation, *J. Mater. Chem. A* 1 (2013) 6350–6358.
- [23] A.L. Ahmad, Z.A. Jawad, S.C. Low, S.H.S. Zein, A cellulose acetate/multi-walled carbon nanotube mixed matrix membrane for CO₂/N₂ separation, *J. Membr. Sci.* 451 (2014) 55–66.
- [24] H. Sanaeepour, A. Kargari, B. Nasernejad, A. Ebadi Amooghini, M. Omidkhah, A novel Co²⁺ exchanged zeolite Y/cellulose acetate mixed matrix membrane for CO₂/N₂ separation, *J. Taiwan Inst. Chem. Eng.* 60 (2016) 403–413.
- [25] D.Q. Vu, W.J. Koros, S.J. Miller, Effect of condensable impurity in CO₂/CH₄ gas feeds on performance of mixed matrix membranes using carbon molecular sieves, *J. Membr. Sci.* 221 (2003) 233–239.
- [26] M. Peydayesh, S. Asarehpour, T. Mohammadi, O. Bakhtiari, Preparation and characterization of SAPO-34 – Matrimid® 5218 mixed matrix membranes for CO₂/CH₄ separation, *Chem. Eng. Res. Des.* 91 (2013) 1335–1342.
- [27] F. Dorosti, M. Omidkhah, R. Abedini, Fabrication and characterization of Matrimid/MIL-53 mixed matrix membrane for CO₂/CH₄ separation, *Chem. Eng. Res. Des.* 92 (2014) 2439–2448.
- [28] A.L. Khan, S.P. Sree, J.A. Martens, M.T. Raza, I.F.J. Vankelecom, Mixed matrix membranes comprising of matrimid and mesoporous COK-12: Preparation and gas separation properties, *J. Membr. Sci.* 495 (2015) 471–478.
- [29] M. Waqas Anjum, B. Bueken, D. De Vos, I.F.J. Vankelecom, MIL-125(Ti) based mixed matrix membranes for CO₂ separation from CH₄ and N₂, *J. Membr. Sci.* 502 (2016) 21–28.
- [30] D.Q. Vu, W.J. Koros, S.J. Miller, Mixed matrix membranes using carbon molecular sieves – I. Preparation and experimental results, *J. Membr. Sci.* 211 (2003) 311–334.
- [31] A.F. Bushell, M.P. Attfield, C.R. Mason, P.M. Budd, Y. Yampolskii, L. Starannikova, A. Reblov, F. Bazzarelli, P. Bernardo, J. Carolus Jansen, M. Lanč, K. Friess, V. Shantarovich, V. Gustov, V. Isaeva, Gas permeation parameters of mixed matrix membranes based on the polymer of intrinsic microporosity PIM-1 and the zeolitic imidazolate framework ZIF-8, *J. Membr. Sci.* 427 (2013) 48–62.
- [32] M.M. Khan, V. Filiz, G. Bengtson, S. Shishatskiy, M.M. Rahman, J. Lillepaerg, V. Abetz, Enhanced gas permeability by fabricating mixed matrix membranes of functionalized multiwalled carbon nanotubes and polymers of intrinsic microporosity (PIM), *J. Membr. Sci.* 436 (2013) 109–120.
- [33] T. Mitra, R.S. Bhavsar, D.J. Adams, P.M. Budd, A.I. Cooper, PIM-1 mixed matrix membranes for gas separations using cost-effective hypercrosslinked nanoparticle fillers, *Chem. Commun.* 52 (2016) 5581–5584.
- [34] N. Tien-Binh, H. Vinh-Thang, X.Y. Chen, D. Rodrigue, S. Kaliaguine, Crosslinked MOF-polymer to enhance gas separation of mixed matrix membranes, *J. Membr. Sci.* 520 (2016) 941–950.
- [35] Z. Tian, S. Wang, Y. Wang, X. Ma, K. Cao, D. Peng, X. Wu, H. Wu, Z. Jiang, Enhanced gas separation performance of mixed matrix membranes from graphitic carbon nitride nanosheets and polymers of intrinsic microporosity, *J. Membr. Sci.* 514 (2016) 15–24.
- [36] H. Wu, X. Li, Y. Li, S. Wang, R. Guo, Z. Jiang, C. Wu, Q. Xin, X. Lu, Facilitated transport mixed matrix membranes incorporated with amine functionalized MCM-41 for enhanced gas separation properties, *J. Membr. Sci.* 465 (2014) 78–90.
- [37] D. Zhao, J. Ren, H. Li, X. Li, M. Deng, Gas separation properties of poly(amide-6-b-ethylene oxide)/amino modified multi-walled carbon nanotubes mixed matrix membranes, *J. Membr. Sci.* 467 (2014) 41–47.
- [38] D. Zhao, J. Ren, H. Li, K. Hua, M. Deng, Poly(amide-6-b-ethylene oxide)/SAPO-34 mixed matrix membrane for CO₂ separation, *J. Energy Chem.* 23 (2014) 227–234.
- [39] G. Dong, J. Hou, J. Wang, Y. Zhang, V. Chen, J. Liu, Enhanced CO₂/N₂ separation by porous reduced graphene oxide/Pebax mixed matrix membranes, *J. Membr. Sci.* 520 (2016) 860–868.
- [40] V. Nafisi, M.-B. Hägg, Development of dual layer of ZIF-8/PEBAX-2533 mixed matrix membrane for CO₂ capture, *J. Membr. Sci.* 459 (2014) 244–255.
- [41] H. Rabiee, S. Meshkat Alasadat, M. Soltanmehr, S.A. Mousavi, A. Ghadimi, Gas permeation and sorption properties of poly(amide-12-b-ethyleneoxide)(Pebax1074)/SAPO-34 mixed matrix membrane for CO₂/CH₄ and CO₂/N₂ separation, *J. Ind. Eng. Chem.* 27 (2015) 223–239.
- [42] S. Zhao, X. Cao, Z. Ma, Z. Wang, Z. Qiao, J. Wang, S. Wang, Mixed-matrix membranes for CO₂/N₂ separation comprising a poly(vinylamine) matrix and metal-organic frameworks, *Ind. Eng. Chem. Res.* 54 (2015) 5139–5148.
- [43] J.Y. Liao, Z. Wang, C.Y. Gao, M. Wang, K. Yan, X.M. Xie, S. Zhao, J.X. Wang, S.C. Wang, A high performance PVAm-HT membrane containing high-speed facilitated transport channels for CO₂ separation, *J. Mater. Chem. A* 3 (2015) 16746–16761.
- [44] A.F. Ismail, P.S. Goh, S.M. Sanip, M. Aziz, Transport and separation properties of carbon nanotube-mixed matrix membrane, *Sep. Purif. Technol.* 70 (2009) 12–26.
- [45] P.S. Goh, A.F. Ismail, S.M. Sanip, B.C. Ng, M. Aziz, Recent advances of inorganic fillers in mixed matrix membrane for gas separation, *Sep. Purif. Technol.* 81 (2011) 243–264.
- [46] D. Bastani, N. Esmaeili, M. Asadollahi, Polymeric mixed matrix membranes containing zeolites as a filler for gas separation applications: A review, *J. Ind. Eng. Chem.* 19 (2013) 375–393.
- [47] I. Erucar, G. Yilmaz, S. Keskin, Recent advances in metal-organic framework-based mixed matrix membranes, *Chem. Asian J.* 8 (2013) 1692–1704.
- [48] B. Seoane, J. Coronas, I. Gascon, M.E. Benavides, O. Karvan, J. Caro, F. Kapteijn, J. Gascon, Metal-organic framework based mixed matrix membranes: A solution for highly efficient CO₂ capture? *Chem. Soc. Rev.* 44 (2015) 2421–2454.
- [49] H.B. Tanh Jeazet, C. Staudt, C. Janiak, Metal-organic frameworks in mixed-matrix membranes for gas separation, *Dalton Trans.* 41 (2012) 14003–14027.
- [50] M. Waqas Anjum, F. de Clippel, J. Didden, A. Laeeq Khan, S. Couck, G.V. Baron, J.F.M. Denayer, B.F. Sels, I.F.J. Vankelecom, Polyimide mixed matrix membranes for CO₂ separations using carbon-silica nanocomposite fillers, *J. Membr. Sci.* 495 (2015) 121–129.
- [51] L. Xiang, Y. Pan, G. Zeng, J. Jiang, J. Chen, C. Wang, Preparation of poly(ether-block-amide)/attapulgite mixed matrix membranes for CO₂/N₂ separation, *J. Membr. Sci.* 500 (2016) 66–75.
- [52] A. Kılıç, Ç. Atalay-Oral, A. Sirkecioglu, Ş.B. Tantekin-Ersolmaz, M.G. Ahunbay, Sod-ZMOF/Matrimid® mixed matrix membranes for CO₂ separation, *J. Membr. Sci.* 489 (2015) 81–89.
- [53] R. Abedini, M. Omidkhah, F. Dorosti, Hydrogen separation and purification with poly (4-methyl-1-pentyne)/MIL 53 mixed matrix membrane based on reverse selectivity, *Int. J. Hydrogen Energy* 39 (2014) 7897–7909.
- [54] T. Rodenas, M. van Dalen, E. García-Pérez, P. Serra-Crespo, B. Zornoza, F. Kapteijn, J. Gascon, Visualizing MOF mixed matrix membranes at the nanoscale: Towards structure-performance relationships in CO₂/CH₄ separation over NH₂-MIL-53(Al)@PI, *Adv. Funct. Mater.* 24 (2014) 249–256.
- [55] M. Naseri, S.F. Mousavi, T. Mohammadi, O. Bakhtiari, Synthesis and gas transport performance of MIL-101/Matrimid mixed matrix membranes, *J. Ind. Eng. Chem.* 29 (2015) 249–256.
- [56] B. Seoane, C. Téllez, J. Coronas, C. Staudt, NH₂-MIL-53(Al) and NH₂-MIL-101(Al) in sulfur-containing copolyimide mixed matrix membranes for gas separation, *Sep. Purif. Technol.* 111 (2013) 72–81.
- [57] T. Rodenas, M. van Dalen, P. Serra-Crespo, F. Kapteijn, J. Gascon, Mixed matrix membranes based on NH₂-functionalized MIL-type MOFs: Influence of structural and operational parameters on the CO₂/CH₄ separation performance, *Microporous Mesoporous Mater.* 192 (2014) 35–42.
- [58] X. Guo, H. Huang, Y. Ban, Q. Yang, Y. Xiao, Y. Li, W. Yang, C. Zhong, Mixed matrix membranes incorporated with amine-functionalized titanium-based metal-organic framework for CO₂/CH₄ separation, *J. Membr. Sci.* 478 (2015) 130–139.
- [59] J. Shen, G. Liu, K. Huang, Q. Li, K. Guan, Y. Li, W. Jin, UiO-66-polyether block amide mixed matrix membranes for CO₂ separation, *J. Membr. Sci.* 513 (2016) 155–165.
- [60] L. Hao, K.-S. Liao, T.-S. Chung, Photo-oxidative PIM-1 based mixed matrix membranes with superior gas separation performance, *J. Mater. Chem. A* 3 (2015) 17273–17281.
- [61] M. Askari, T.-S. Chung, Natural gas purification and olefin/paraffin separation using thermal cross-linkable co-polyimide/ZIF-8 mixed matrix membranes, *J. Membr. Sci.* 444 (2013) 173–183.
- [62] V. Nafisi, M.-B. Hägg, Gas separation properties of ZIF-8/6FDA-durene diamine mixed matrix membrane, *Sep. Purif. Technol.* 128 (2014) 31–38.
- [63] W.S. Chi, S. Hwang, S.-J. Lee, S. Park, Y.-S. Bae, D.Y. Ryu, J.H. Kim, J. Kim, Mixed matrix membranes consisting of SEBS block copolymers and size-controlled ZIF-8 nanoparticles for CO₂ capture, *J. Membr. Sci.* 495 (2015) 479–488.
- [64] S. Hwang, W.S. Chi, S.J. Lee, S.H. Im, J.H. Kim, J. Kim, Hollow ZIF-8 nanoparticles improve the permeability of mixed matrix membranes for CO₂/CH₄ gas separation, *J. Membr. Sci.* 480 (2015) 11–19.
- [65] A. Ehsani, M. Pakizeh, Synthesis, characterization and gas permeation study of ZIF-11/Pebax® 2533 mixed matrix membranes, *J. Taiwan Inst. Chem. Eng.* 66 (2016) 414–423.
- [66] X. Li, L. Ma, H. Zhang, S. Wang, Z. Jiang, R. Guo, H. Wu, X. Cao, J. Yang, B. Wang, Synergistic effect of combining carbon nanotubes and graphene oxide in mixed matrix membranes for efficient CO₂ separation, *J. Membr. Sci.* 479 (2015) 1–10.
- [67] L. Dong, M. Chen, J. Li, D. Shi, W. Dong, X. Li, Y. Bai, Metal-organic framework-graphene oxide composites: a facile method to highly improve the CO₂ separation performance of mixed matrix membranes, *J. Membr. Sci.* 520 (2016) 801–811.
- [68] J. Zhao, Z. Wang, J. Wang, S. Wang, High-performance membranes comprising polyaniline nanoparticles incorporated into polyvinylamine matrix for CO₂/N₂ separation, *J. Membr. Sci.* 403–404 (2012) 203–215.
- [69] S. Zhao, Z. Wang, Z. Qiao, X. Wei, C. Zhang, J. Wang, S. Wang, Gas separation membrane with CO₂-facilitated transport highway constructed from amino carrier containing nanorods and macromolecules, *J. Mater. Chem. A* 1 (2013) 246–249.
- [70] X. Li, M. Wang, S. Wang, Y. Li, Z. Jiang, R. Guo, H. Wu, X. Cao, J. Yang, B. Wang, Constructing CO₂ transport passageways in Matrimid® membranes using nanohydrogels for efficient carbon capture, *J. Membr. Sci.* 474 (2015) 156–166.
- [71] X. Li, Z. Jiang, Y. Wu, H. Zhang, Y. Cheng, R. Guo, H. Wu, High-performance composite membranes incorporated with carboxylic acid nanogels for CO₂ separation, *J. Membr. Sci.* 495 (2015) 72–80.

- [72] S. Wang, Z. Tian, J. Feng, H. Wu, Y. Li, Y. Liu, X. Li, Q. Xin, Z. Jiang, Enhanced CO₂ separation properties by incorporating poly(ethylene glycol)-containing polymeric submicrospheres into polyimide membrane, *J. Membr. Sci.* 473 (2015) 310–317.
- [73] L.M. Robeson, Polymer blends in membrane transport processes, *Ind. Eng. Chem. Res.* 49 (2010) 11859–11865.
- [74] H.A. Mannan, H. Mukhtar, T. Murugesan, R. Nasir, D.F. Mohshim, A. Mushtaq, Recent applications of polymer blends in gas separation membranes, *Chem. Eng. Technol.* 36 (2013) 1838–1846.
- [75] M. Wang, Z. Wang, N. Li, J. Liao, M. S. Zhao, J. Wang, S. Wang, Relationship between polymer–filler interfaces in separation layers and gas transport properties of mixed matrix composite membranes, *J. Membr. Sci.* 495 (2015) 252–268.
- [76] H. Sanaeepur, A. Kargari, B. Nasernejad, Aminosilane-functionalization of a nanoporous Y-type zeolite for application in a cellulose acetate based mixed matrix membrane for CO₂ separation, *RSC Adv.* 4 (2014) 63966–63976.
- [77] A. Ebadi Amooghin, M. Omidkhah, A. Kargari, The effects of aminosilane grafting on NaY zeolite–Matrimid® 5218 mixed matrix membranes for CO₂/CH₄ separation, *J. Membr. Sci.* 490 (2015) 364–379.
- [78] M. Laghaei, M. Sadeghi, B. Ghalei, M. Shahrooz, The role of compatibility between polymeric matrix and silane coupling agents on the performance of mixed matrix membranes: Polyethersulfone/MCM-41, *J. Membr. Sci.* 513 (2016) 20–32.
- [79] L. Dong, C. Zhang, Y. Bai, D. Shi, X. Li, H. Zhang, M. Chen, High-performance PEBA2533-functional MMT mixed matrix membrane containing high-speed facilitated transport channels for CO₂/N₂ separation, *ACS Sustain. Chem. Eng.* 4 (2016) 3486–3496.
- [80] B. Zornoza, C. Téllez, J. Coronas, O. Esekhi, W.J. Koros, Mixed matrix membranes based on 6FDA polyimide with silica and zeolite microsphere dispersed phases, *AIChE J.* 61 (2015) 4481–4490.
- [81] M. Loloei, M. Omidkhah, A. Moghadassi, A.E. Amooghin, Preparation and characterization of Matrimid® 5218 based binary and ternary mixed matrix membranes for CO₂ separation, *Int. J. Greenhouse Gas Control* 39 (2015) 225–235.
- [82] Y.C. Hudiono, T.K. Carlisle, J.E. Bara, Y. Zhang, D.L. Gin, R.D. Noble, A three-component mixed-matrix membrane with enhanced CO₂ separation properties based on zeolites and ionic liquid materials, *J. Membr. Sci.* 350 (2010) 117–123.
- [83] Y.C. Hudiono, T.K. Carlisle, A.L. LaFratre, D.L. Gin, R.D. Noble, Novel mixed matrix membranes based on polymerizable room-temperature ionic liquids and SAPO-34 particles to improve CO₂ separation, *J. Membr. Sci.* 370 (2011) 141–148.
- [84] L. Hao, P. Li, T. Yang, T.-S. Chung, Room temperature ionic liquid/ZIF-8 mixed-matrix membranes for natural gas sweetening and post-combustion CO₂ capture, *J. Membr. Sci.* 436 (2013) 221–231.
- [85] C. Casado-Coterillo, A. Fernandez-Barquin, B. Zornoza, C. Tellez, J. Coronas, A. Irabien, Synthesis and characterisation of MOF/ionic liquid/chitosan mixed matrix membranes for CO₂/N₂ separation, *RSC Adv.* 5 (2015) 102350–102361.
- [86] H. Li, L. Tuo, K. Yang, H.-K. Jeong, Y. Dai, G. He, W. Zhao, Simultaneous enhancement of mechanical properties and CO₂ selectivity of ZIF-8 mixed matrix membranes: Interfacial toughening effect of ionic liquid, *J. Membr. Sci.* 511 (2016) 130–142.
- [87] Q. Xin, J. Ouyang, T. Liu, Z. Li, Z. Li, Y. Liu, S. Wang, H. Wu, Z. Jiang, X. Cao, Enhanced interfacial interaction and CO₂ separation performance of mixed matrix membrane by incorporating polyethylenimine-decorated metal–organic frameworks, *ACS Appl. Mater. Interfaces* 7 (2015) 1065–1077.
- [88] X. Li, Y. Cheng, H. Zhang, S. Wang, Z. Jiang, R. Guo, H. Wu, Efficient CO₂ capture by functionalized graphene oxide nanosheets as fillers to fabricate multi-permselective mixed matrix membranes, *ACS Appl. Mater. Interfaces* 7 (2015) 5528–5537.
- [89] R. Lin, L. Ge, L. Hou, E. Strounina, V. Rudolph, Z. Zhu, Mixed matrix membranes with strengthened MOFs/polymer interfacial interaction and improved membrane performance, *ACS Appl. Mater. Interfaces* 6 (2014) 5609–5618.
- [90] Z. Wang, D. Wang, S. Zhang, L. Hu, J. Jin, Interfacial design of mixed matrix membranes for improved gas separation performance, *Adv. Mater.* 28 (2016) 3399–3405.
- [91] S. Shahid, K. Nijmeijer, S. Nehache, I. Vankelecom, A. Deratani, D. Quemener, MOF-mixed matrix membranes: Precise dispersion of MOF particles with better compatibility via a particle fusion approach for enhanced gas separation properties, *J. Membr. Sci.* 492 (2015) 21–31.
- [92] N. Tien-Binh, H. Vinh-Thang, X.Y. Chen, D. Rodrigue, S. Kaliaguine, Polymer functionalization to enhance interface quality of mixed matrix membranes for high CO₂/CH₄ gas separation, *J. Mater. Chem. A* 3 (2015) 15202–15213.
- [93] Ekiner, O.M., Kulkarni, S.S., Process for making hollow fiber mixed matrix membranes, U.S. Patent 6663805, 2003.
- [94] L.Y. Jiang, T.S. Chung, C. Cao, Z. Huang, S. Kulprathipanja, Fundamental understanding of nano-sized zeolite distribution in the formation of the mixed matrix single- and dual-layer asymmetric hollow fiber membranes, *J. Membr. Sci.* 252 (2005) 89–100.
- [95] L.Y. Jiang, T.S. Chung, S. Kulprathipanja, An investigation to revitalize the separation performance of hollow fibers with a thin mixed matrix composite skin for gas separation, *J. Membr. Sci.* 276 (2006) 113–125.
- [96] Y. Li, T. Chung, Z. Huang, S. Kulprathipanja, Dual-layer polyethersulfone (PES)/BTDA-TDI/MDI co-polyimide (P84) hollow fiber membranes with a submicron PES–zeolite beta mixed matrix dense-selective layer for gas separation, *J. Membr. Sci.* 277 (2006) 28–37.
- [97] L.Y. Jiang, T.S. Chung, S. Kulprathipanja, Fabrication of mixed matrix hollow fibers with intimate polymer–zeolite interface for gas separation, *AIChE J.* 52 (2006) 2898–2908.
- [98] H.Z. Chen, Y.C. Xiao, T.-S. Chung, Multi-layer composite hollow fiber membranes derived from poly(ethylene glycol) (PEG) containing hybrid materials for CO₂/N₂ separation, *J. Membr. Sci.* 381 (2011) 211–220.
- [99] D.F. Li, T.-S. Chung, R. Wang, Y. Liu, Fabrication of fluoropolyimide/polyethersulfone (PES) dual-layer asymmetric hollow fiber membranes for gas separation, *J. Membr. Sci.* 198 (2002) 211–223.
- [100] S. Kulprathipanja, J. Charoenphol, Mixed matrix membrane for separation of gases, U.S. Patents 6726744B2, 2004.
- [101] S. Kulprathipanja, J. Soontraratpong, J.J. Chiou, Mixed matrix membrane for gas separation, U.S. Patents 7344585B1, 2008.
- [102] F. de Clippel, A.L. Khan, A. Cano-Odena, M. Dusselier, K. Vanherck, L. Peng, S. Oswald, L. Giebeler, S. Corthals, B. Kenens, J.F.M. Denayer, P.A. Jacobs, I.F.J. Vankelecom, B.F. Sels, CO₂ reverse selective mixed matrix membranes for H₂ purification by incorporation of carbon–silica fillers, *J. Mater. Chem. A* 1 (2013) 945–953.
- [103] J. Wang, Y. Li, Z. Zhang, Z. Hao, Mesoporous KIT-6 silica-polydimethylsiloxane (PDMS) mixed matrix membranes for gas separation, *J. Mater. Chem. A* 3 (2015) 8650–8658.
- [104] M.M. Khan, V. Filiz, G. Bengtson, S. Shishatskiy, M. Rahman, V. Abetz, Functionalized carbon nanotubes mixed matrix membranes of polymers of intrinsic microporosity for gas separation, *Nanoscale Res. Lett.* 7 (2012) 1–12.
- [105] E. Ahmadpour, M.V. Sarfaraz, R.M. Behbahani, A.A. Shamsabadi, M. Aghajani, Fabrication of mixed matrix membranes containing TiO₂ nanoparticles in Pebax 1657 as a copolymer on an ultra-porous PVC support, *J. Nat. Gas Sci. Eng.* 35 (Part A) (2016) 33–41.
- [106] Y. Shen, H. Wang, X. Zhang, Y. Zhang, MoS₂ nanosheets functionalized composite mixed matrix membrane for enhanced CO₂ capture via surface drop-coating method, *ACS Appl. Mater. Interfaces* 8 (2016) 23371–23378.
- [107] K. Zarshenas, A. Raisi, A. Aroujalian, Mixed matrix membrane of nano-zeolite NaX/poly (ether-block-amide) for gas separation applications, *J. Membr. Sci.* 510 (2016) 270–283.
- [108] T. Li, Y. Pan, K.-V. Peinemann, Z. Lai, Carbon dioxide selective mixed matrix composite membrane containing ZIF-7 nano-fillers, *J. Membr. Sci.* 425–426 (2013) 235–242.
- [109] A. Jomekian, R.M. Behbahani, T. Mohammadi, A. Kargari, CO₂/CH₄ separation by high performance co-casted ZIF-8/Pebax 1657/PES mixed matrix membrane, *J. Nat. Gas Sci. Eng.* 31 (2016) 562–574.
- [110] J. Kim, Q. Fu, J.M.P. Scofield, S.E. Kentish, G.G. Qiao, Ultra-thin film composite mixed matrix membranes incorporating iron(III)-dopamine nanoparticles for CO₂ separation, *Nano* 8 (2016) 8312–8323.
- [111] W. Salim, W.S.W. Ho, Recent developments on nanostructured polymer-based membranes, *Curr. Opin. Chem. Eng.* 8 (2015) 76–82.
- [112] X. Yu, Z. Wang, J. Zhao, F. Yuan, S. Li, J. Wang, S. Wang, An effective method to improve the performance of fixed carrier membrane via incorporation of CO₂-selective adsorptive silica nanoparticles, *Chin. J. Chem. Eng.* 19 (2011) 821–832.
- [113] J.Y. Liao, Z. Wang, C.Y. Gao, S.C. Li, Z.H. Qiao, M. Wang, S. Zhao, X.M. Xie, J.X. Wang, S.C. Wang, Fabrication of high-performance facilitated transport membranes for CO₂ separation, *Chem. Sci.* 5 (2014) 2843–2849.
- [114] Z. Qiao, S. Zhao, J. Wang, S. Wang, M.D. Guiver, A highly permeable aligned montmorillonite mixed-matrix membrane for CO₂ separation, *Angew. Chem. Int. Ed.* 55 (2016) 9321–9325.
- [115] X. Cao, Z. Qiao, Z. Wang, S. Zhao, P. Li, J. Wang, S. Wang, Enhanced performance of mixed matrix membrane by incorporating a highly compatible covalent organic framework into poly(vinylamine) for hydrogen purification, *Int. J. Hydrogen Energy* 41 (2016) 9167–9174.
- [116] L. Deng, M.-B. Hägg, Carbon nanotube reinforced PVAm/PVA blend FSC nanocomposite membrane for CO₂/CH₄ separation, *Int. J. Greenhouse Gas Control* 26 (2014) 127–134.
- [117] Y. Shen, H. Wang, J. Liu, Y. Zhang, Enhanced performance of a novel polyvinyl amine/chitosan/graphene oxide mixed matrix membrane for CO₂ capture, *ACS Sustain. Chem. Eng.* 3 (2015) 1819–1829.
- [118] R. Xing, W.S.W. Ho, Crosslinked polyvinylalcohol–polysiloxane/fumed silica mixed matrix membranes containing amines for CO₂/H₂ separation, *J. Membr. Sci.* 367 (2011) 91–102.
- [119] Y. Zhao, B.T. Jung, L. Ansaloni, W.S.W. Ho, Multiwalled carbon nanotube mixed matrix membranes containing amines for high pressure CO₂/H₂ separation, *J. Membr. Sci.* 459 (2014) 233–243.
- [120] L. Ansaloni, Y. Zhao, B.T. Jung, K. Ramasubramanian, M.G. Baschetti, W.S.W. Ho, Facilitated transport membranes containing amino-functionalized multi-walled carbon nanotubes for high-pressure CO₂ separations, *J. Membr. Sci.* 490 (2015) 18–28.
- [121] R.D. Noble, Perspectives on mixed matrix membranes, *J. Membr. Sci.* 378 (2011) 393–397.